Subcritical bifurcation of shear-thinning plane Poiseuille flows

A. CHEKILA[1,2], C. NOUAR[2], E. PLAUT[2] AND A. NEMDILI[1]

[1]Laboratoire de Rhéologie, Faculté de Génie Mécanique, Université des Sciences et de la Technologie d'Oran, Algérie

[2]LEMTA, UMR 7563 (CNRS- Nancy Université), 2 Avenue de la Forêt de Haye, BP 160, 54504 Vandoeuvre Cedex, France

(Received ?? and in revised form ??)

In a recent article (Nouar *et al.* 2007), a linear stability analysis of plane Poiseuille flow of shear-thinning fluids has been performed. The authors concluded that the viscosity stratification delays the transition and that is important to account for the viscosity perturbation. The current paper focuses on the first principles understanding of the influence of the viscosity stratification and the nonlinear variation of the effective viscosity μ with the shear rate $\dot{\gamma}$ on the flow stability with respect to a finite amplitude perturbation. A weakly nonlinear analysis, using the amplitude expansion method is adopted as a first approach to study nonlinear effects. The bifurcation to two-dimensional travelling waves is studied. For the numerical computations, the shear-thinning behavior is described by the Carreau model. The rheological parameters are varied in a wide range. The results indicate that (i) the nonlinearity of the viscous terms tends to reduce the viscous dissipation and to accelerate the flow, (ii) the harmonic generated by the nonlinearity $\mu(\dot{\gamma})$ is smaller and in opposite phase with that generated by the quadratic nonlinear inertial terms and (iii) with increasing shear-thinning effects, the bifurcation becomes highly subcritical. Consequently, the magnitude of the threshold amplitude of the perturbation,

beyond which the flow is nonlinearly unstable, decreases. This result is confirmed by computing higher order Landau constants.

---

1. Introduction

Non-Newtonian fluid flows occur in many industrial processes. The control of these processes requires knowledge of the flow structure and in particular of the conditions for stability and transition to turbulence. Most non-Newtonian fluids have two common properties: viscoelasticity and shear-thinning. This theoretical work is related to the shear flow stability of purely viscous shear-thinning fluids, i.e., fluids without elastic response and for which the effective viscosity $\hat{\mu}$ decreases with increasing shear rate. Flows of these fluids are mainly characterized by a viscosity stratification in the direction normal to the wall. It has been shown by several authors that the stability characteristics of parallel shear flows can be significantly modified by such a viscosity stratification, which can also be obtained when the viscosity $\hat{\mu}$ depends on an intensive quantity obeying an advection-diffusion equation. Wall & Wilson (1996) considered the stability of plane channel flow of a Newtonian fluid with temperature-dependent viscosity, the walls being maintained at different temperatures. Four different viscosity models were considered. They found that a non-uniform increase of the viscosity in the channel always stabilizes the flow, whereas a non-uniform decrease in the channel may either destabilize or stabilize the flow. These results were explained in terms of three physical effects, namely bulk effect due to uniform increase or decrease of viscosity, a velocity-profile shape effect as the basic velocity profile becomes non-symmetrical and a thin-layer effect when a thin layer of lower or higher viscosity develops adjacent to a channel wall. The influence of heating on the stability of channel flow was also recently addressed by Sameen & Govindarajan

(2007). They showed that a decrease in viscosity towards the wall stabilizes the flow. The effect of viscosity stratification on the stability of plane channel flow with respect to infinitesimal perturbations has been also analyzed by Ranganathan & Govindarajan (2001), Govindarajan (2002), Govindarajan *et al.* (2003) and Chikkadi *et al.* (2005). They showed that any viscosity profile in the critical layer, in which the viscosity decreases towards the wall, delays significantly the onset of two-dimensional modes. This effect was related to a reduced energy intake from the mean flow to the fluctuations. The energy dissipation responds less drastically to changes in viscosity. It was then argued that similar physics should hold in the case of turbulent drag reduction by polymers additive, when the production layer overlaps the viscosity-stratified layer.

Recently, Nouar *et al.* (2007) investigated the linear stability of viscously stratified channel flow, focusing on shear-thinning fluids modeled by the Carreau rheological law. The degree of stabilization observed is more modest than the prediction of Chikkadi *et al.* (2005). The disagreement stems from the neglect of the viscosity perturbation in Chikkadi *et al.* (2005), Govindarajan *et al.* (2001), Govindarajan *et al.* (2003). When it is taken into account the fluctuating shear-stress tensor becomes anisotropic (Nouar *et al.* 2007). Indeed, denoting by x and y the streamwise and wall-normal directions, the xy-component of the viscous stress tensor perturbation implies the tangent viscosity, which is smaller than the effective viscosity. The other components of the viscous stress tensor perturbation are proportional to the effective viscosity (see equations 2.24, 2.25 and 2.30 below). In the studies described above, the influence of the viscosity stratification on the stability of plane channel flow has been described in the framework of linear stability analysis. It is natural to inquire if the stabilizing effects observed in the linear regime exist also in the nonlinear regime. Here, we seek a first-principles understanding of the influence of the viscosity stratification and the nonlinear variation of the effective viscosity $\hat{\mu}$ with

the shear rate $\hat{\dot{\gamma}}$ on the flow stability in the presence of finite amplitude disturbances. A weakly nonlinear analysis is used as a first approach to take into account nonlinear effects. These effects will be analyzed through (i) the nature of the bifurcation, (ii) the modification of the base flow, (iii) the generated harmonic and (iv) the threshold amplitude of the perturbation which limits the basin of attraction of the laminar parallel flow. To our knowledge, the weakly nonlinear stability analysis of shear-thinning fluid flow in a plane channel has not been performed so far. For such non Newtonian fluids, the viscous term in the momentum equation, which is linear (proportional to the Laplacian of the velocity) in Newtonian fluids, becomes highly nonlinear. In fact, Govindarajan *et al.* (2003) studied the effect of viscosity stratification on the development of secondary instabilities, i.e. three dimensional linear instabilities of finite amplitude Tollmien-Schlichting waves. The authors found a strong stabilization. The secondary instabilities modes are slaved by the primary mode and are rapidly damped. In this study, the authors did not include the viscosity fluctuation in the stability equations. This can be justified if an infinite scalar coefficient diffusion is considered for the perturbation. This assumption is, however, incompatible with a laminar steady viscosity profile (Ern *et al.* 2003). Taking into account the viscosity perturbation may modify the conclusions drawn by the authors.

Here, we consider only the case of shear-thinning behavior, i.e. the case where $\hat{\mu}$ decreases as the shear rate increases. Particulate dispersions, polymer colloids and polymer solutions can display this behavior above a certain concentration threshold. For polymer solutions, the shear-thinning phenomenon arises because the dissolved macromolecules form aggregates via hydrogen bonds and polymer chain entanglement, which are progressively disrupted under the influence of increasing shear rate (Phillips & Williams 2000). In addition, the individual polymer network may align in the direction of the flow, reducing further the energy dissipated under shear. For suspension of particles, the mechanism

of shear-thinning is described for instance in Quemada (1978). The choice of a suitable constitutive model is not crucial at this stage: all the analytical relations are given for a general nonlinear purely viscous fluid. For the numerical applications, we adopt the Carreau (1972) model. This model has been chosen because it has a sound theoretical basis and is frequently adopted to describe the rheological behavior of shear-thinning fluids. Stability analysis data are also available in the literature for this fluid model.

This article is organized as follows. In §2 we formulate the physical problem, state the governing equations and define the dimensionless parameters. The velocity and viscosity profiles of the base state are discussed and the disturbance equations are derived. Subsequently, the linearization of the disturbance equations and the eigenvalue problem derivation for the linear stability analysis are presented in §3. In §4, the weakly nonlinear scheme is described in detail as well as the method of determination of the Landau constant. Section 5 presents and discusses the numerical results focusing on the influence of the shear-thinning behavior of the fluid. Finally, §6 summarizes the salient conclusions of the present study.

2. Poiseuille flows of shear-thinning fluids

2.1. *Governing equations - Dimensionless parameters*

We consider the flow of a shear-thinning incompressible fluid between two plates at $\hat{y} = \pm\,\hat{h}$. A constant pressure gradient $\dfrac{\partial \hat{P}}{\partial \hat{x}}$ is imposed in the streamwise direction $\boldsymbol{e}_x$. The wall-normal direction is defined by the unit vector $\boldsymbol{e}_y$. Here and in what follows, the quantities with hat ($\hat{.}$) are dimensional. Distances are scaled with $\hat{h}$, velocity with the maximal velocity $\hat{U}_0$ of the base flow, time with $\dfrac{\hat{h}}{\hat{U}_0}$, pressure and stresses with $\hat{\rho}\,\hat{U}_0^2$.

Using these scales, the governing equations in dimensionless form are:

$$\boldsymbol{\nabla}.\boldsymbol{U} = 0, \tag{2.1}$$

$$\frac{\partial \boldsymbol{U}}{\partial t} + (\boldsymbol{U}.\boldsymbol{\nabla})\,\boldsymbol{U} = -\boldsymbol{\nabla} P + \boldsymbol{\nabla}.\boldsymbol{\tau}, \tag{2.2}$$

where $\boldsymbol{U} = U\boldsymbol{e}_x + V\boldsymbol{e}_y$ denotes the fluid velocity, P the pressure (incorporating gravity effects) and $\boldsymbol{\tau}$ the deviatoric stress tensor. The fluid is supposed to be purely viscous, i.e., its viscosity depends only on the shear rate. The constitutive equation reads:

$$\boldsymbol{\tau} = \frac{1}{Re}\,\mu\,(\Gamma)\,\dot{\boldsymbol{\gamma}} \qquad \text{with} \qquad \dot{\boldsymbol{\gamma}} = \boldsymbol{\nabla}\boldsymbol{U} + (\boldsymbol{\nabla}\boldsymbol{U})^T\,. \tag{2.3}$$

Here, Re is the Reynolds number defined as:

$$Re = \frac{\hat{\rho}\,\hat{U}_0\,\hat{h}}{\hat{\mu}_0}, \tag{2.4}$$

$\dot{\boldsymbol{\gamma}}$ is the rate-of-strain tensor and Γ its second invariant:

$$\Gamma = \frac{1}{2}\,\dot{\gamma}_{ij}\,\dot{\gamma}_{ij}. \tag{2.5}$$

For the numerical applications, the viscosity $\hat{\mu}$ is given by the Carreau model (Bird *et al.* 1987),

$$\frac{\hat{\mu} - \hat{\mu}_\infty}{\hat{\mu}_0 - \hat{\mu}_\infty} = \left(1 + \hat{\lambda}^2\,\hat{\Gamma}\right)^{\frac{n_c - 1}{2}}, \tag{2.6}$$

where $\hat{\mu}_0$ and $\hat{\mu}_\infty$ are the viscosities at low and high shear rate, $n_c < 1$ the shear-thinning index, $\hat{\lambda}$ the characteristic time of the fluid. The location of the transition from the Newtonian plateau to the shear-thinning regime is determined by $\hat{\lambda}$, since $1/\hat{\lambda}$ defines the characteristic shear rate for the onset of shear-thinning. Increasing $\hat{\lambda}$ reduces the Newtonian plateau to lower shear rates. The infinite-shear-rate viscosity is generally associated with a breakdown of the fluid, and is frequently significantly smaller (10^{-3} to 10^{-4} times smaller) than $\hat{\mu}_0$, see Bird *et al.* (1987) and Tanner (2000). The ratio $\hat{\mu}_\infty/\hat{\mu}_0$

will be thus neglected in the following. The dimensionless effective viscosity is then

$$\mu = \frac{\hat{\mu}}{\hat{\mu}_0} = \left(1 + \lambda^2\,\Gamma\right)^{\frac{n_c-1}{2}} \quad \text{with} \quad \lambda = \frac{\hat{\lambda}}{\hat{h}/\hat{U}_0} = \frac{\hat{\lambda}}{\hat{\rho}\,\hat{h}^2/\hat{\mu}_0}\,Re = \Lambda\,Re, \tag{2.7}$$

where $1/\lambda$ is the dimensionless characteristic shear rate for the onset of shear-thinning and Λ the ratio of the characteristic time of the fluid to the viscous diffusion time. This ratio Λ is fixed for a given fluid and flow geometry. The Newtonian behavior, $\hat{\mu} = \hat{\mu}_0$, is obtained by setting $n_c = 1$ or $\hat{\lambda} = 0$. If $\hat{\Gamma} >> 1/\hat{\lambda}^2$, the Carreau model reduces to the power-law model $\hat{\mu} = \hat{K}\hat{\Gamma}^{\frac{n_c-1}{2}}$ with a consistency $\hat{K} = \hat{\mu}_0\,\hat{\lambda}^{n_c-1}$.

2.2. *Base flows*

The base flow is parallel and steady: $\boldsymbol{U}_b = U_b(y)\,\boldsymbol{e}_x$ and $P_b = P_b(x)$. The momentum equation reduces to

$$0 = -\frac{dP_b}{dx} + \frac{1}{Re}\,\frac{d}{dy}\left(\mu_b \frac{dU_b}{dy}\right) \tag{2.8}$$

with

$$\mu_b = \left(1 + \lambda^2 \left(\frac{dU_b}{dy}\right)^2\right)^{\frac{n_c-1}{2}}.$$

The subscript b refers to the base flow. Numerical solutions of (2.8) are required, since this equation is nonlinear. An iterative spectral method is used for this purpose. Examples of the basic velocity, $U_b(y)$, and the viscosity profile, $\mu_b(y)$, are given in figures 1 and 2 for various values of the parameters λ and n_c. As expected, the velocity profiles flatten with increasing shear-thinning and the wall axial velocity gradients increase thereby reducing the wall shear-viscosity. The figure 2 shows that both decreasing n_c and increasing λ have the effect of increasing shear-thinning in the fluid, but in two distinct ways. For fixed n_c, increasing λ to large values drives an increase of the viscosity-gradient $|d\mu_b/dy|$ near the axis, and its decrease near the wall (figure 2a). Vice-versa, when λ is fixed and n_c is decreased (figure 2b). Because of the crucial role of the viscosity stratification

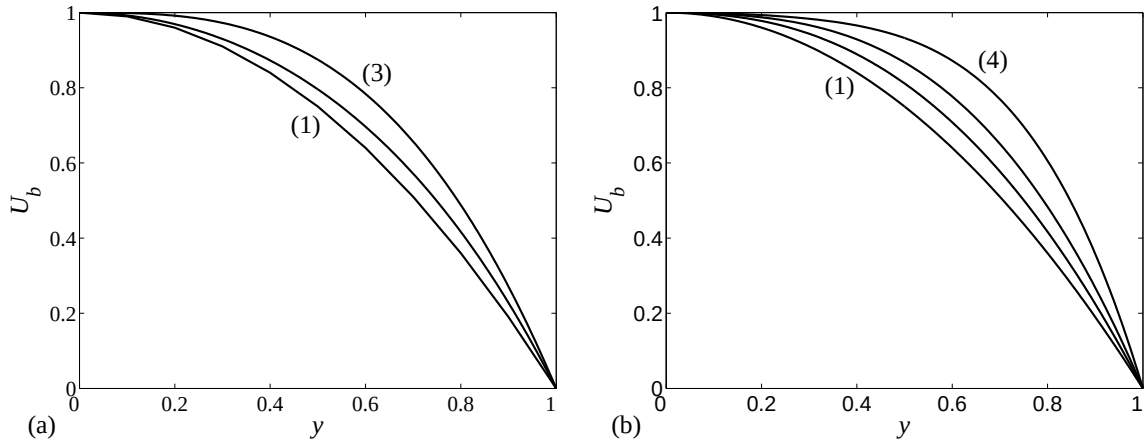

FIGURE 1. Basic velocity profiles: **(a)** $n_c = 0.5$ and different values of λ: (1) $\lambda = 0$ Newtonian; (2) $\lambda = 1$; (3) $\lambda = 100$. **(b)** $\lambda = 10$ and different values of n_c: (1) $n_c = 1$ Newtonian; (2) $n_c = 0.7$; (3) $n_c = 0.5$; (4) $n_c = 0.3$.

in the critical layer, in the linear stability analysis, we have represented in figure 3 the wall viscosity-gradient $|d\mu_b/dy|_w$ as function of the rheological parameters n_c and λ. From $\lambda = 0$, *i.e.*, Newtonian case, $|d\mu_b/dy|_w$ increases sharply, reaches a maximum at $\lambda \approx 1$ and then decreases with increasing λ. It can be shown using (2.7) that when $\lambda >> 1$, $(d\mu_b/dy)_w \approx (n_c - 1)\,\lambda^{n_c-1}\,(\Gamma_b)_w^{n_c-1}\,(d\Gamma_b/dy)_w$, where $(\Gamma_b)_w$ and $(d\Gamma_b/dy)_w$ can be calculated analytically using power-law model. Thus, $|d\mu_b/dy|_w$ decreases as λ^{n_c-1}. However, one should take care of the fact that $(\mu_b)_w$ also decreases with increasing λ. It appears therefore more appropriate to consider the ratio $\left(\frac{1}{\mu_b}\left|\frac{d\mu_b}{dy}\right|\right)$ as function of the rheological parameters. This ratio is called here the degree of viscosity stratification and denoted Sv. Figure 3(b) shows that $(Sv)_w$ increases with increasing shear-thinning effects. For $\lambda >> 1$, $(Sv)_w$ saturates to a constant value identical to that calculated for a power-law fluid, i.e., $(1 - n_c)/n_c$.

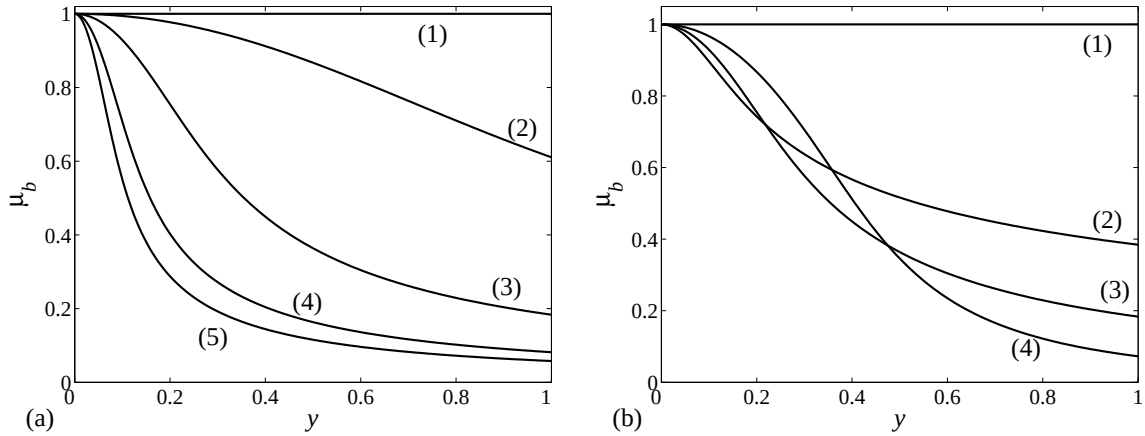

FIGURE 2. Basic viscosity profiles: **(a)** $n_c = 0.5$ and different values of λ: (1) $\lambda = 0$ Newtonian; (2) $\lambda = 1$; (3) $\lambda = 10$; (4) $\lambda = 50$; (5) $\lambda = 100$. **(b)** $\lambda = 10$ and different values of n_c: (1) $n_c = 1$ Newtonian; (2) $n_c = 0.7$; (3) $n_c = 0.5$; (4) $n_c = 0.3$.

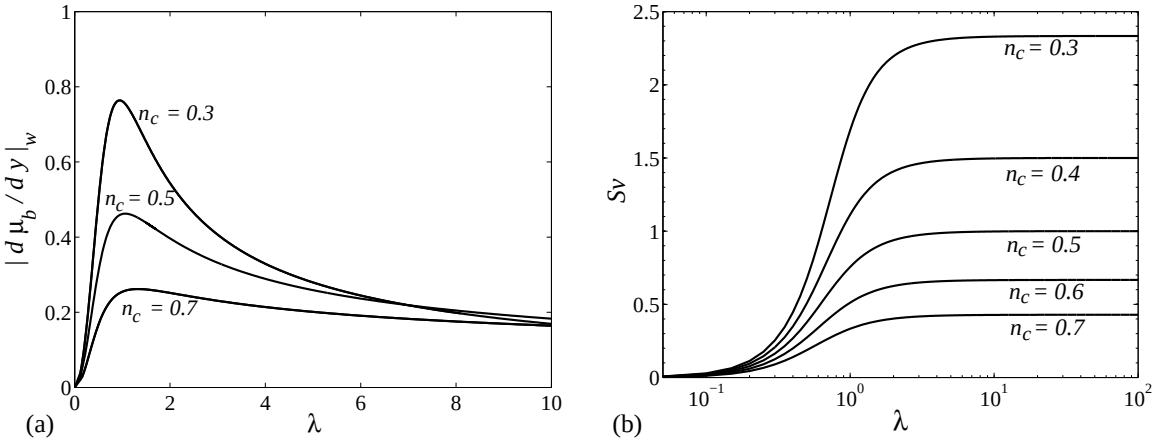

FIGURE 3. (a) Wall viscosity-gradient as function of the rheological parameters. (b) Degree of viscosity stratification Sv at the wall as function of the rheological parameters.

2.3. *Disturbance equations*

The velocity $\boldsymbol{U}$ and pressure P of the disturbed flow are split into the basic field (with subscript b) and the disturbance:

$$\boldsymbol{U} = \boldsymbol{U}_b + \boldsymbol{u}, \quad P = P_b + p. \tag{2.9}$$

Here, we consider two-dimensional disturbances in the $(x,\, y)$-plane added to the basic field. It is worthy to note that there is no equivalent of Squire's theorem for nonlinear viscous fluids. However, the numerical tests performed in Nouar & Frigaard (2009), for a large range of rheological parameters and of streamwise and spanwise wave numbers, show that the lowest critical Reynolds number is obtained for spanwise homogeneous perturbation. This result could be anticipated since the viscosity felt by the perturbation in two-dimensional situation (tangent viscosity) is less than that in three-dimensional situation, as it also indicated in equation (2.25) below.

We introduce the streamfunction for the disturbance, $\psi(x, y; t)$, such that

$$u = \frac{\partial \psi}{\partial y}, \quad v = -\frac{\partial \psi}{\partial x}. \tag{2.10}$$

The equation governing the stream function of an unsteady disturbance is obtained by cross-differentiating $x-$ and $y-$ momentum equations and eliminating the pressure. This yields the vorticity equation,

$$\begin{aligned} \frac{\partial}{\partial t}\Delta\psi = \left(D^2 U_b - U_b\,\Delta\right)\frac{\partial \psi}{\partial x} + J(\psi, \Delta\,\psi) + \frac{\partial^2}{\partial x \partial y}\left[\tau_{xx}\left(\Psi_b + \psi\right) - \tau_{yy}\left(\Psi_b + \psi\right)\right] \\ + \left(\frac{\partial^2}{\partial y^2} - \frac{\partial^2}{\partial x^2}\right)\tau_{xy}\left(\Psi_b + \psi\right) \end{aligned} \tag{2.11}$$

where $D \equiv d/dy$, Ψ_b is the stream function associated with the base flow $U_b = D\Psi_b$, $J\,(f, g)$ is the Jacobian defined by $(\partial f/\partial x)\,(\partial g/\partial y) - (\partial f/\partial y)\,(\partial g/\partial x)$, $\Delta \equiv \partial^2/\partial x^2 + \partial^2/\partial y^2$ and $\tau_{ij}\left(\Psi_b + \psi\right) = \mu\left(\Psi_b + \psi\right)\dot{\gamma}_{ij}\left(\Psi_b + \psi\right)$. No-slip boundary conditions are imposed at the walls:

$$\frac{\partial \psi}{\partial x} = \frac{\partial \psi}{\partial y} = 0 \quad \text{at} \quad y = \pm 1. \tag{2.12}$$

For a small amplitude disturbance, the viscosity of the perturbed flow can be expanded around the base flow as:

$$\mu(\Psi_b + \psi) = \mu_b + \mu_1\,(\psi) + \mu_2\,(\psi,\, \psi) + \mu_3\,(\psi,\, \psi,\, \psi) + ..., \tag{2.13}$$

where

$$\mu_1(\psi) = \left.\frac{\partial\mu}{\partial\dot{\gamma}_{ij}}\right|_b \dot{\gamma}_{ij}(\psi), \tag{2.14}$$

$$\mu_2(\psi,\psi) = \frac{1}{2}\left.\frac{\partial^2\mu}{\partial\dot{\gamma}_{ij}\,\partial\dot{\gamma}_{k\ell}}\right|_b \dot{\gamma}_{ij}(\psi)\,\dot{\gamma}_{k\ell}(\psi), \tag{2.15}$$

$$\mu_3(\psi,\psi,\psi) = \frac{1}{6}\left.\frac{\partial^3\mu}{\partial\dot{\gamma}_{ij}\,\partial\dot{\gamma}_{k\ell}\,\partial\dot{\gamma}_{pq}}\right|_b \dot{\gamma}_{ij}(\psi)\,\dot{\gamma}_{k\ell}(\psi)\,\dot{\gamma}_{pq}(\psi). \tag{2.16}$$

The deviatoric stresses in the disturbed flow can also be written as

$$\tau_{ij}(\Psi_b+\psi) = \tau_{ij}(\Psi_b) + \tau_{1,ij}(\psi) + \tau_{2,ij}(\psi,\psi) + \tau_{3,ij}(\psi,\psi,\psi) + ..., \tag{2.17}$$

with

$$\tau_{1,ij}(\psi) = \frac{1}{Re}\left[\mu_1(\psi)\;\dot{\gamma}_{ij}(\Psi_b) + \mu_b\,\dot{\gamma}_{ij}(\psi)\right], \tag{2.18}$$

$$\tau_{2,ij}(\psi,\psi) = \frac{1}{Re}\left[\mu_2(\psi,\psi)\;\dot{\gamma}_{ij}(\Psi_b) + \mu_1(\psi)\;\dot{\gamma}_{ij}(\psi)\right], \tag{2.19}$$

$$\tau_{3,ij}(\psi,\psi,\psi) = \frac{1}{Re}\left[\mu_3(\psi,\psi,\psi)\;\dot{\gamma}_{ij}(\Psi_b) + \mu_2(\psi,\psi)\;\dot{\gamma}_{ij}(\psi)\right]. \tag{2.20}$$

In the following, $A_1(\psi)$, $A_2(\psi,\psi)$ and $A_3(\psi,\psi,\psi)$ where A stands for τ_{ij} or μ, will be denoted respectively A_1, A_2 and A_3. In the base flow $\dot{\gamma}^b_{ij} = \dot{\gamma}_{ij}(\Psi_b) = 0$ if $ij \neq xy, yx$ and $\dot{\gamma}^b_{ij} = DU_b$ if $ij = xy, yx$. Setting $\Gamma_b = (DU_b)^2$ and $\Gamma_2 = (1/2)\,\dot{\gamma}_{ij}(\psi)\,\dot{\gamma}_{ij}(\psi)$, the expressions of μ_1, μ_2 and μ_3 can be simplified,

$$\mu_1 = 2\left.\frac{\partial\mu}{\partial\Gamma}\right|_b \dot{\gamma}^b_{xy}\,\dot{\gamma}_{xy}(\psi), \tag{2.21}$$

$$\mu_2 = \left.\frac{\partial\mu}{\partial\Gamma}\right|_b \Gamma_2 + 2\left.\frac{\partial^2\mu}{\partial\Gamma^2}\right|_b \Gamma_b\,\dot{\gamma}^2_{xy}(\psi), \tag{2.22}$$

$$\mu_3 = 2\left.\frac{\partial^2\mu}{\partial\Gamma^2}\right|_b \dot{\gamma}^b_{xy}\,\dot{\gamma}_{xy}(\psi)\;\Gamma_2 + \frac{4}{3}\left.\frac{\partial^3\mu}{\partial\Gamma^3}\right|_b \left(\dot{\gamma}^b_{xy}\right)^3 \dot{\gamma}^3_{xy}(\psi). \tag{2.23}$$

Replacing μ_1, μ_2 and μ_3 by their corresponding expressions (2.21)-(2.23) into eqs. (2.18)-(2.20) we obtain

$$\tau_{1,ij} = \frac{1}{Re}\,\mu_b \dot{\gamma}_{ij}\,(\psi) \quad \text{if} \quad ij \neq xy,\, yx, \tag{2.24}$$

$$\tau_{1,xy} = \tau_{1,yx} = \frac{1}{Re}\,\left[\mu_b + 2\,\Gamma_b\,\left.\frac{\partial \mu}{\partial \Gamma}\right|_b\right]\dot{\gamma}_{xy}\,(\psi) = \frac{1}{Re}\,\mu_t \dot{\gamma}_{xy}\,(\psi)\,, \tag{2.25}$$

$$\tau_{2,ij} = \frac{1}{Re}\,\mu_1\,\dot{\gamma}_{ij}\,(\psi) \qquad \text{if} \qquad ij \neq xy,\, yx, \tag{2.26}$$

$$\tau_{2,xy} = \frac{1}{Re}\,\left[\,\mu_1\,\dot{\gamma}_{xy}\,(\psi) + \mu_2\,\dot{\gamma}_{xy}\,(\Psi_b)\,\right], \tag{2.27}$$

$$\tau_{3,ij} = \frac{1}{Re}\,\mu_2\,\dot{\gamma}_{ij}\,(\psi) \qquad \text{if} \qquad ij \neq xy, yx, \tag{2.28}$$

$$\tau_{3,xy} = \frac{1}{Re}\,\left[\,\mu_2\,\dot{\gamma}_{xy}\,(\psi) + \mu_3\,\dot{\gamma}_{xy}\,(\Psi_b)\,\right]. \tag{2.29}$$

In equation (2.25),

$$\mu_t = \mu_b + 2\Gamma_b\,\left.\frac{\partial \mu}{\partial \Gamma}\right|_b \tag{2.30}$$

is the tangent viscosity, which can be also defined by $\mu_t = (\partial \tau_{xy}/\partial \dot{\gamma}_{xy})_b$. For shear-thinning fluid, $\mathrm{d}\mu_b/\mathrm{d}\Gamma < 0$ and $\mu_t < \mu_b$. Finally, the disturbance equation (2.11) can be rewritten

$$\frac{\partial}{\partial t}\Delta\psi = \mathcal{L}\,(\psi) + \mathcal{N}\,(\psi)\,. \tag{2.31}$$

The linear and nonlinear terms of (2.11) are gathered in $\mathcal{L}\,(\psi)$ and $\mathcal{N}\,(\psi)$ respectively, where we separate the contributions of the inertial and viscous terms as follows:

$$\mathcal{L} = \mathcal{L}_I + \mathcal{L}_{V1} + \mathcal{L}_{V2} + \mathcal{L}_{V3}, \tag{2.32}$$

$$\mathcal{N} = \mathcal{N}_I + \mathcal{N}_{Vquad} + \mathcal{N}_{Vcub} + ..., \tag{2.33}$$

with

$$\mathcal{L}_I(\psi) = \left(D^2 U_b - U_b\,\Delta\right)\frac{\partial\psi}{\partial x}, \tag{2.34}$$

$$Re\;\mathcal{L}_{V1}(\psi) = \mu_b\,\Delta^2(\psi), \tag{2.35}$$

$$Re\;\mathcal{L}_{V2}(\psi) = \left(D^2\mu_b\right)\dot{\gamma}_{xy}(\psi) + D\mu_b\left[2\frac{\partial\dot{\gamma}_{xy}}{\partial y}(\psi) + \frac{\partial\dot{\gamma}_{xx}}{\partial x}(\psi) - \frac{\partial\dot{\gamma}_{yy}}{\partial x}(\psi)\right], \tag{2.36}$$

$$Re\;\mathcal{L}_{V3}(\psi) = \left(\frac{\partial^2}{\partial y^2} - \frac{\partial^2}{\partial x^2}\right)\left[(\mu_t - \mu_b)\,\dot{\gamma}_{xy}(\psi)\right], \tag{2.37}$$

$$\mathcal{N}_I(\psi,\psi) = J(\psi,\Delta\psi), \tag{2.38}$$

$$\begin{aligned} Re\;\mathcal{N}_{Vquad}(\psi,\psi) = {} & \frac{\partial^2}{\partial x\partial y}\left[\mu_1\,\left(\dot{\gamma}_{xx}(\psi) - \dot{\gamma}_{yy}(\psi)\right)\right] \\ & + \left(\frac{\partial^2}{\partial y^2} - \frac{\partial^2}{\partial x^2}\right)\left[\mu_1\dot{\gamma}_{xy}(\psi) + \mu_2\,\dot{\gamma}_{xy}(\Psi_b)\right], \end{aligned} \tag{2.39}$$

$$\begin{aligned} Re\;\mathcal{N}_{Vcub}(\psi,\psi,\psi) = {} & \frac{\partial^2}{\partial x\partial y}\left[\mu_2\,\left(\dot{\gamma}_{xx}(\psi) - \dot{\gamma}_{yy}(\psi)\right)\right] \\ & + \left(\frac{\partial^2}{\partial y^2} - \frac{\partial^2}{\partial x^2}\right)\left[\mu_2\dot{\gamma}_{xy}(\psi) + \mu_3\,\dot{\gamma}_{xy}(\Psi_b)\right]. \end{aligned} \tag{2.40}$$

The subscripts I and V refer to inertial and viscous terms. $\mathcal{L}_{V1}$ is a "Newtonian-like" viscous term, $\mathcal{L}_{V2}$ and $\mathcal{L}_{V3}$ reflect respectively the spatial stratification of the viscosity and the anisotropy of the deviatoric shear-stress tensor perturbation. $\mathcal{N}_I$ is the nonlinear inertial term. $\mathcal{N}_{Vquad}$ and $\mathcal{N}_{Vcub}$ gather the quadratic and cubic terms which arise from the nonlinear variation of the effective viscosity with the shear rate. Higher order expansions, up to seventh order, are given in Appendix C

3. Linear stability analysis

3.1. *Direct problem*

To solve the linearized version of the disturbance equation (2.31), we use the normal mode analysis, assuming that

$$\psi(x,y;t) = f_{1,1}(y)\exp\left[i\alpha\,(x - c\,t)\right] \tag{3.1}$$

with α the axial wave number and $c = c_r + i\,c_i$ the complex wave speed. Its real part c_r is the phase velocity and the imaginary part yields the growth rate $\alpha\, c_i$. It can be shown that $f_{1,1}(y)$ satisfies the modified Orr-Sommerfeld equation

$$L_1\, f_{1,1} = 0 \tag{3.2}$$

with

$$L_1 \equiv -i\,\alpha\, c\, S_1 \,+\, i\,\alpha\, \left[U_b\, S_1 - D^2 U_b\right] \,-\, \frac{1}{Re}\left[\mu_b\, S_1^2 + 2\,(D\mu_b)\; S_1\, D + \left(D^2\mu_b\right)\; \mathcal{G}_1\,\right] - \frac{1}{Re}\mathcal{G}_1\left[(\mu_t - \mu_b)\,\mathcal{G}_1\,\right]. \tag{3.3}$$

The operators S_n and $\mathcal{G}_n$ are defined by

$$S_n \equiv D^2 - n^2\,\alpha^2 \qquad \text{and} \qquad \mathcal{G}_n \equiv D^2 + n^2\,\alpha^2 \quad , \quad n \geqslant 1. \tag{3.4}$$

The boundary conditions are

$$f_{1,1} = Df_{1,1} = 0 \quad \text{at} \quad y = \pm 1. \tag{3.5}$$

The eigenvalue problem (3.2)-(3.5) is invariant with respect to the symmetry $y \mapsto -y$, therefore the eigenmodes are either odd or even under $y \mapsto -y$. We consider only the eigenmodes which are unstable at the lowest Reynolds number, which appear to be the *even* modes as in the Newtonian case (Drazin & Reid 1995). The boundary conditions at $y = -1$ can therefore be replaced by the parity conditions:

$$Df_{1,1} = D^3 f_{1,1} = 0 \quad \text{at} \quad y = 0. \tag{3.6}$$

Since any multiple of an eigenfunction is also a solution of (3.2), $f_{1,1}$ can be normalized according to

$$f_{1,1} = 1 \quad \text{at} \quad y = 0, \tag{3.7}$$

which fixes amplitude and phase of the wave (3.1). The eigenvalue problem (3.2) with its boundary conditions is solved using Chebychev collocation method, see e.g. Schmid &

Henningson (2001). The characteristics of the destabilizing waves and the critical parameters α_c, c_c and Re_c (critical wavenumber, critical phase velocity and critical Reynolds number) will be given in §5.1, after the presentation of the weakly nonlinear analysis.

3.2. *Adjoint problem*

The adjoint operator of L_1, equation (3.2), is defined with the hermitian inner product, $(f,g) = \displaystyle\int_0^1 f(y)\, g^*(y)\, dy$, between two functions $f(y)$ and $g(y)$ of $H^2([0,1])$. The homogeneous adjoint problem associated to the equation (3.2) is given as

$$L_1^\dagger f_{1,1}^\dagger = 0, \tag{3.8}$$

with

$$L_1^\dagger \equiv i\,\alpha\, c^\dagger\, S_1 - i\,\alpha\, \left[U_b\, S_1 + 2\, (DU_b)\, D\right] - \frac{1}{Re}\left[\mu_b\, S_1^2 + 2\,(D\mu_b)\, S_1\, D + \left(D^2\mu_b\right)\, \mathcal{G}_1\right]$$
$$- \frac{1}{Re}\mathcal{G}_1\, \left[(\mu_t - \mu_b)\, \mathcal{G}_1\right] \tag{3.9}$$

and

$$Df_{1,1}^\dagger = D^3 f_{1,1}^\dagger = 0 \quad \text{at} \quad y = 0 \qquad ; \qquad f_{1,1}^\dagger = Df_{1,1}^\dagger = 0 \quad \text{at} \quad y = 1. \tag{3.10}$$

4. Weakly nonlinear analysis

4.1. *General asymptotic expansion - Landau equation*

Once the critical parameters are known, in order to study the saturation of the bifurcation to the waves, a weakly nonlinear analysis is used. Due to the nonlinear terms in the disturbance equation (2.31), it is clear that a nonlinear solution which contains the fundamental mode in $\exp\left[\pm i\alpha_c\,(x - c_c t)\right]$ must also contain harmonic modes in $\exp\left[ni\alpha_c\,(x - c_c\, t)\right]$ for all n integers. Therefore, it seems natural to represent the nonlinear disturbance as the

Fourier series

$$\psi\,(x,\,y,\,t) = \phi_0(y,t) + \sum_{\substack{n=-\infty \\ n\neq 0}}^{+\infty} \phi_n\,(y,t)\,\exp\left[ni\alpha_c\,(x - c_c t)\right], \tag{4.1}$$

where we have separated out the mean part $\phi_0(y,t)$, *i.e.* the mean flow distortion. Because ψ is real, we have that $\phi_{-n} = \phi_n^*$, where the star denotes complex conjugation. Substituting (4.1) into (2.31) combined with (2.32)-(2.40) and (2.21)-(2.23) and separating out the coefficients of like exponentials, we obtain an infinite set of coupled nonlinear partial differential equations for the Fourier components ϕ_n. The nonlinearity and coupling of this infinite set makes its solution difficult. However, if the amplitude A of the fundamental wave is small, the Fourier components ϕ_n can be sought using a perturbation method expanding around the solution of the linear problem. It is clear that if the linear solution is $O(A)$, the leading term of ϕ_2 is $O(A^2)$ because of the interaction of the fundamental with itself. The same reasoning applied for higher harmonics indicate that ϕ_n can be written as

$$\phi_n(y,\,t) = A^n(t) f_n(y,t) \quad \text{if} \quad n > 0 \quad \text{and} \quad \phi_0(y,\,t) = |A|^2 f_0(y,t), \tag{4.2}$$

with

$$f_n(y,t) = \sum_{m=1}^{+\infty} |A|^{2(m-1)} f_{n,n+2(m-1)}(y) \quad \text{if} \quad n \neq 0 \tag{4.3}$$

$$f_0(y,t) = \sum_{m=1}^{+\infty} |A|^{2(m-1)} f_{0,2m}(y), \tag{4.4}$$

see e.g. Watson (1960); Stuart (1960); Reynolds & Potter (1967); Herbert (1983). In the above equations, $A = A(t)$ is the complex amplitude of the fundamental, described as a general function of time and considered as a small parameter. The subscripts to function $f_{k,\ell}$ means that it has an harmonic index k and asymptotic order ℓ.

The time evolution of the disturbance amplitude A is given by the Stuart-Landau equa-

tion:

$$\frac{dA}{dt} = -i\alpha\ (c - c_c)\ A + \sum_{j=1}^{+\infty} g_j\, |A|^{2j}\, A, \tag{4.5}$$

where c is the complex phase velocity evaluated in the vicinity of the critical conditions $c = c\,(\alpha_c, Re)$ and g_j is jth Landau coefficient. This is in fact a rigorous series expansion in powers of A at the onset, i.e., for $c = c_c$, but it is customary to truncate the series at a finite order, and to use the Landau equation (4.5) at a finite distance of the onset. As A is assumed complex, the real amplitude is given by the the modulus of the amplitude A which is determined by:

$$\frac{d\,|A|^2}{dt} \ = \ 2\alpha\, c_i\ |A|^2 + 2\ \sum_{j=1}^{+\infty} g_{jr}\ |A|^{2(j+1)}\,, \tag{4.6}$$

where the subscript jr in g_{jr} means the real part of g_j. For linearly unstable flows, the nature of the bifurcation is determined g_{1r}. If g_{1r} is positive, then the instability is subcritical, while if g_{1r} is negative, the instability is supercritical. The imaginary part g_{1i} gives the first order correction to the frequency of the basic wave due to nonlinear effects.

In the system of equations obtained after substituting (4.1) into (2.31) and separating terms of like exponential, the Fourier components ϕ_n are replaced by their expression (4.2) combined with (4.3)-(4.5). Equating the same powers A, a hierarchy of ordinary differential equations for the functions $f_{k,\ell}$ is obtained. These are solved sequentially beginning from $k = 1, \ell = 1$. The problem $k = 1$, $\ell = 1$ is the linear problem (3.2) which gives the critical point around which the harmonic-amplitude expansion is carried out. The problem $k = 0$, $\ell = 2$ yields the first correction to the mean flow. The problem $k = 2$, $\ell = 2$ yields the first harmonic of the fundamental mode. The problem $k = 1$, $\ell = 3$ yields the coefficient g_1 of feedback on the fundamental mode.

In order to avoid overloading the text, the linear (L_k), bilinear (N_I and N_{Vquad}) and

trilinear forms (N_{Vcub}), involved in the ordinary differential equations for the functions $f_{k,\ell}$, are given in Appendix A.

4.2. *Modification of the mean flow*

The interaction of the fundamental mode $Af_{1,1}$ with its complex conjugate produces a mean flow correction proportional to $|A|^2$, *i.e.*, $|A|^2 u_{0,2}$, where $u_{0,2} = Df_{0,2}$. Actually, this modification of the mean flow cannot be calculated using the vorticity equation (2.31), since, in this x-independent case, the linear operator implied is not invertible. Instead, one has to consider the streamwise mean momentum equation. In the situation of a fixed axial pressure gradient, it reduces to:

$$\left\langle \frac{\partial}{\partial y}\left(uv\right)\right\rangle_x = \left\langle \frac{\partial}{\partial y}\tau_{1,xy}\right\rangle_x + \left\langle \frac{\partial}{\partial y}\tau_{2,xy}\right\rangle_x , \tag{4.7}$$

where $\langle . \rangle_x = \dfrac{\alpha}{2\pi}\displaystyle\int_0^{2\pi/\alpha} (.)dx$. Using (2.25) , (2.27) and (2.22), it can be shown after some algebra, that u_{02} satisfies the following equation:

$$\begin{aligned}\frac{1}{Re} D\left(\mu_t\, Du_{0,2}\right) = & -i\alpha D\left(f_{1,1}Df_{1,1}^* - f_{1,1}^* Df_{1,1}\right) \\ & - \frac{2}{Re} D\left[\dot{\gamma}_{xy}^b \left.\frac{\partial \mu}{\partial \Gamma}\right|_b \left(3\,|\,\mathcal{G}_1 f_{1,1}\,|^2 + 4\alpha^2 |\,Df_{1,1}\,|^2\right)\right] \\ & - \frac{4}{Re} D\left[\dot{\gamma}_{xy}^b\, \Gamma_b \left.\frac{\partial^2 \mu}{\partial \Gamma^2}\right|_b |\,\mathcal{G}_1 f_{1,1}\,|^2\right].\end{aligned} \tag{4.8}$$

with the boundary and parity conditions

$$u_{0,2} = 0 \quad \text{at} \quad y = 1 \qquad \text{and} \quad Du_{0,2} = 0 \quad \text{at} \quad y = 0 \tag{4.9}$$

4.3. *Generation of the first harmonic of the fundamental mode*

The interaction of the fundamental with itself, through the quadratic nonlinear terms of the perturbations equation, produces first harmonic term, $f_{2,2}A^2E^2$. At order $k = 2$, $\ell = 2$, the perturbation equation (2.31) combined with (4.2)-(4.5) reduces to:

$$L_2\, f_{2,2} = N_I\left(f_{1,1}, f_{1,1}\right) + N_{Vquad}\left(f_{1,1}, f_{1,1}\right). \tag{4.10}$$

The boundary and parity conditions read

$$f_{2,2} = Df_{2,2} = 0 \quad \text{at} \quad y = 1 \qquad \text{and} \qquad f_{2,2} = D^2 f_{2,2} = 0 \quad \text{at} \quad y = 0. \tag{4.11}$$

4.4. *Calculation of the cubic Landau constant*

The cubic Landau constant g_1 appears in the problem $k = 1, \ell = 3$. This problem represents the feedback at order $O(A^3)$ on the fundamental mode through the nonlinear interactions of the fundamental with the first harmonic and with the modification of the mean flow. It reads:

$$\begin{aligned} L_1 f_{1,3} = -g_1\, S_1\, f_{1,1} &+ N_I\left(f_{0,2}|f_{1,1}\right) + N_{Vquad}\left(f_{0,2}|f_{1,1}\right) \\ &+ N_I\left(f_{2,2}|f_{-1,1}\right) + N_{Vquad}\left(f_{2,2}|f_{-1,1}\right) \\ &+ N_{Vcub}\left(f_{1,1}, f_{1,1}|f_{-1,1}\right), \end{aligned} \tag{4.12}$$

where $f_{-k,\ell} = f^*_{k,\ell}$. In the critical conditions, equation (4.12) has a non trivial solution if the Fredholm solvability condition is satisfied, i.e., orthogonality of the inhomogeneous part of the equation (4.12) to the null-space of the adjoint operator of L_1, see §3.2. The cubic Landau coefficient is then readily obtained,

$$g_1 = g_1^I + g_1^V = \left(g_{10}^I + g_{12}^I\right) + \left(g_{10}^V + g_{12}^V + g_{1-11}^V\right), \tag{4.13}$$

with

$$g_{10}^I = \frac{\left(N_I(f_{0,2}|f_{1,1}), f_{1,1}^\dagger\right)}{\left(S_1 f_{1,1},\, f_{1,1}^\dagger\right)} \quad , \quad g_{10}^V = \frac{\left(N_{Vquad}(f_{0,2}|f_{1,1}), f_{1,1}^\dagger\right)}{\left(S_1 f_{1,1},\, f_{1,1}^\dagger\right)}, \tag{4.14}$$

$$g_{12}^I = \frac{\left(N_I(f_{2,2}, |f_{-1,1}), f_{1,1}^\dagger\right)}{\left(S_1 f_{1,1},\, f_{1,1}^\dagger\right)} \quad , \quad g_{12}^V = \frac{\left(N_{Vquad}(f_{2,2}|f_{-1,1}), f_{1,1}^\dagger\right)}{\left(S_1 f_{1,1},\, f_{1,1}^\dagger\right)}, \tag{4.15}$$

$$g_{1-11}^V = \frac{\left(N_{Vcub}(f_{1,1}, f_{1,1}|f_{-1,1}), f_{1,1}^\dagger\right)}{\left(S_1 f_{1,1},\, f_{1,1}^\dagger\right)}, \tag{4.16}$$

where g_{10}^I and g_{10}^V are the feedback of the mean flow correction onto the wave through the nonlinear inertial and nonlinear viscous terms, g_{12}^I is the feedback of the harmonic onto the wave, etc...

5. Results and discussion

5.1. *Linear problem*

A spectral collocation method based on Chebyshev polynomials is applied to determine the eigenvalues c and the corresponding eigenfunctions. The differential equation (3.2) combined with (3.3) is discretized on the Gauss-Lobatto grid. The resulting generalized eigenvalue problem is solved using the QZ algorithm with Matlab. Spectra with increasing collocation points ($N = 50$, 100, 150, 200, 300) were compared to determine the adequate number $(N + 1)$ of Chebyshev polynomials. It is found that, in order to keep the same resolution accuracy (within five digits) of the least stable mode for all the situations considered here, it is necessary to increase N as the shear-thinning behavior of the fluid becomes more important. For instance, $N = 200$ for a Carreau fluid with $n_c = 0.1$ and $\lambda = 10$, whilst $N = 50$ in the Newtonian case. Marginal stability curves and the associated critical conditions are determined for different rheological parameters (n_c, λ). To determine the critical conditions, for a given rheological parameters, α and Re are varied until $c_i \leqslant 10^{-5}$. Numerical results have been already given in (Nouar *et al.* 2007). When the Reynolds number is defined with the wall-shear viscosity

$$Re_{cw} = Re_c / \left(\mu_b\right)_w , \tag{5.1}$$

the shear-thinning delays the linear instability as shown in Table 1. The results of Nouar *et al.* (2007) are supplemented here by additional data for large values of λ and another shear-thinning index n_c. In figure 4, the critical Reynolds number Re_{cw} is depicted vs

n_c	λ	Re_{cw}	α_c	c_c
1	0	5772.22	1.0206	$2.640\,10^{-1}$
0.7	10	9257.62	0.995	$2.308\,10^{-1}$
0.5	10	13849.66	1.009	$2.070\,10^{-1}$
0.3	10	23519.04	1.1043	$1.810\,10^{-1}$
0.5	1	13225.62	0.9333	$2.004\,10^{-1}$
0.5	100	13732.71	1.013	$2.0861\,10^{-1}$

TABLE 1. Critical Reynolds number Re_{cw}, critical wavenumber α_c and critical wave speed c_c for various rheological parameters.

λ for different values of n_c. The stabilizing effect of the shear-thinning is clearly illustrated. One has also to note, that the evolution of Re_{cw} v.s. the rheological parameters is correlated to that of the degree of viscosity stratification at the wall, *i.e.*, $\dfrac{1}{\mu_b}\,|D\mu_b|$ at $y = 1$ (see figure 3b). The evolution of the critical wavenumber with the shear-thinning behavior has been described in (Nouar *et al.* 2007). At large λ and when n_c is decreased, the waves have a shorter wavelength, and also a lower phase speed (Table 1).

Remark

Note that, if the perturbation of the viscosity is not taken into account, *i.e.*, one sets $\mu_t = \mu_b$ in (3.3), the stabilizing effect is much stronger. The critical Reynolds number is 2 to 3 times higher.

Some characteristics of the critical wave are shown in figure 5 for Newtonian and Carreau fluids. For such fluids, the streamlines are more concentrated near the wall, indicating the presence of steep velocity gradient and a large unaffected core region.

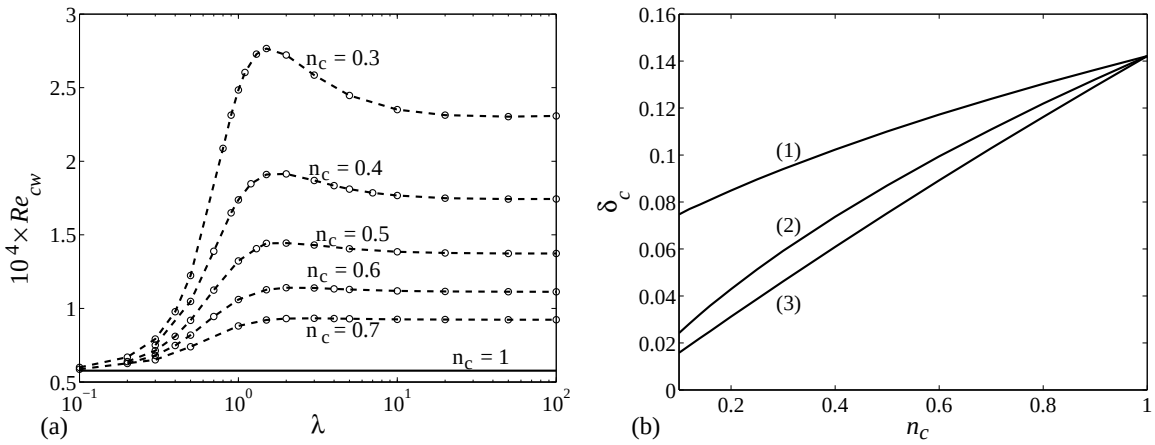

FIGURE 4. **(a)** Critical Reynolds number defined with the wall shear viscosity as function of the dimensionless characteristic time λ of the fluid for different values of n_c. **(b)** Thickness of the critical layer as function of n_c for different λ: (1) $\lambda = 0.5$; (2) $\lambda = 1$; (3) $\lambda = 10$.

The slope of the separatrices (lines where the stream function vanishes) near the wall is related to the energy exchange between the mean flow and the disturbance. It has been shown (Plaut *et al.* 2008) that for the disturbance to extract energy from the basic flow through the action of the Reynolds stress, the separatrices must slope against the mean flow. The thickness δ_c of the critical layer, where the exchange of energy between the perturbation and the base flow takes place, is represented as function of n_c for different λ, in figure 4(b). The critical layer becomes thinner when the shear-thinning effects increase. The structure of the critical eigenfunctions is depicted in figure 6 for $\lambda = 10$ and different values of n_c and in figure 7 for $n_c = 0.5$ and different λ. Concerning the critical eigenfunctions of the adjoint linear operator, they are given in Appendix B for various values of the shear-thinning index.

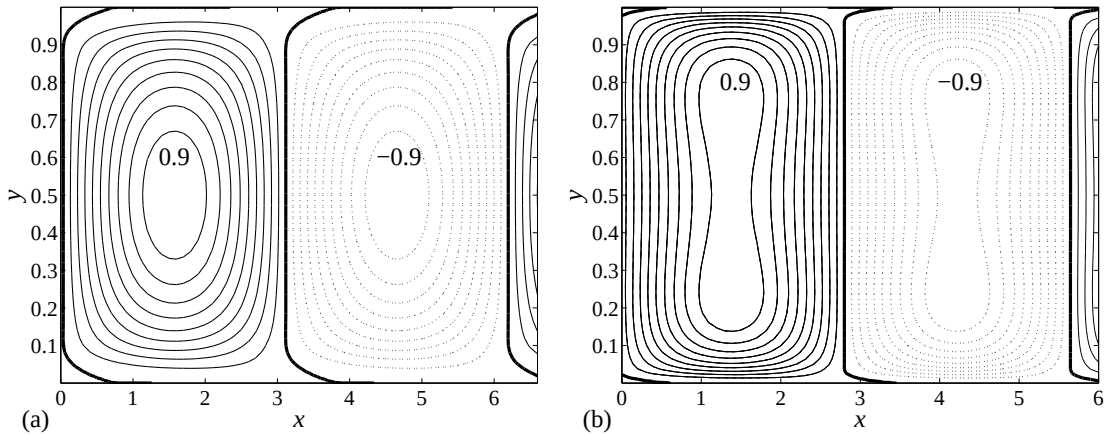

FIGURE 5. Iso-values of the streamfunction associated with the critical waves. **(a)** Newtonian fluid; **(b)** Carreau fluid with $\lambda = 10$ and $n_c = 0.3$: Continuous lines for positive values of ψ: 0.1 near the walls then with a step of 0.1 until 0.9. Dotted lines for negative values of ψ: -0.1 near the walls then with a step of -0.1 until -0.9. The thick lines are the separatrices where the stream-function vanishes.

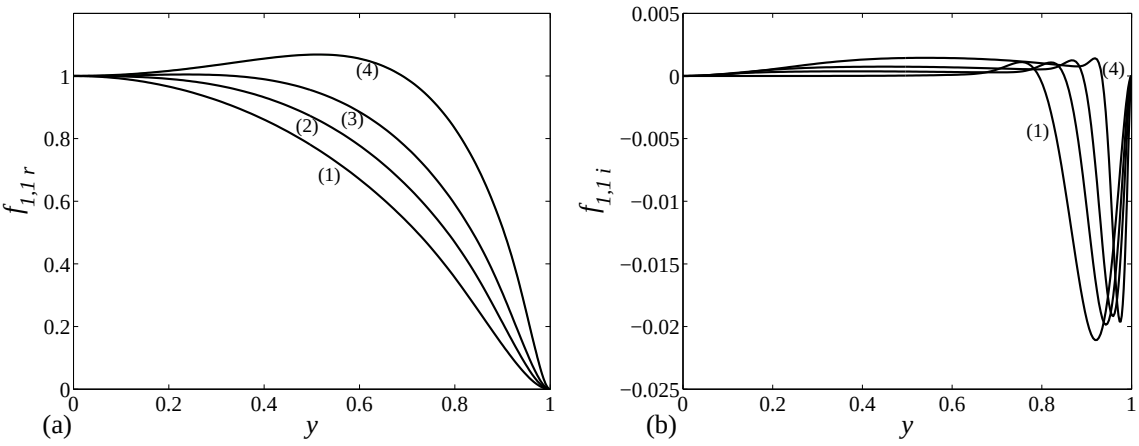

FIGURE 6. **(a)** Real part, **(b)** imaginary part of the eigenfunctions associated to the critical mode for $\lambda = 10$ and different values of the shear-thinning index n_c: (1) $n_c = 1$, Newtonian; (2) $n_c = 0.7$; (3) $n_c = 0.5$; (4) $n_c = 0.3$.

5.2. *Energy equation*

To analyze the importance of the viscosity perturbation on the critical Reynolds number, it is useful to consider the Reynolds-Orr energy equation truncated at order $|A|^2$,

$$\frac{1}{2}\frac{d}{dt}\left\langle u_1^2 + v_1^2 \right\rangle_{xy} = -\frac{1}{Re}\left\langle \mu_b \boldsymbol{\nabla}(\boldsymbol{v}_1) : \boldsymbol{\nabla}(\boldsymbol{v}_1) \right\rangle_{xy} - \left\langle u_1 v_1 \frac{dU_b}{dy} \right\rangle_{xy} + \frac{1}{Re}\left\langle (\mu_b - \mu_t)\left(\dot{\gamma}_{xy}\right)^2 \right\rangle_{xy} \tag{5.2}$$

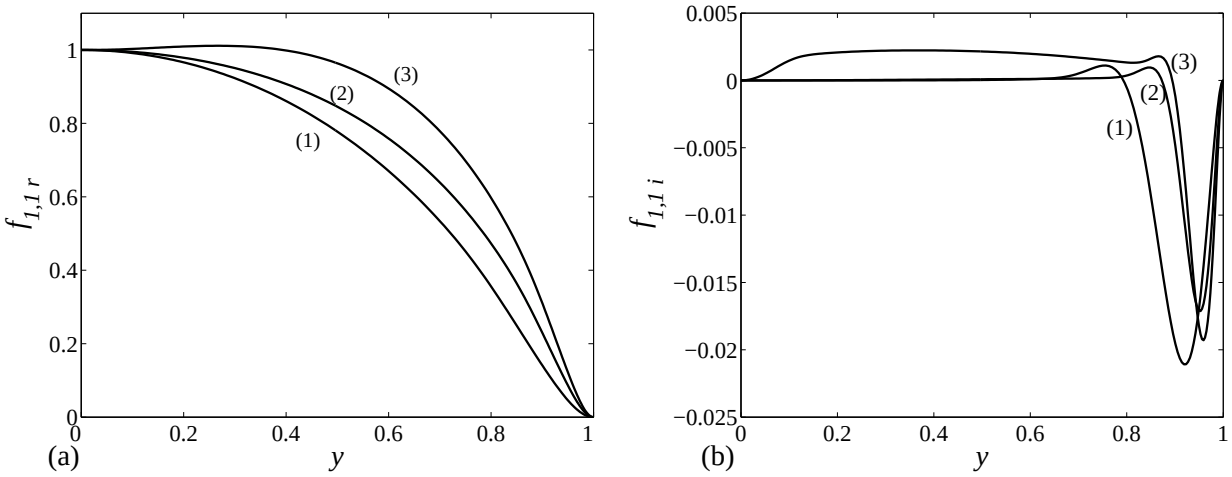

FIGURE 7. **(a)** Real part, **(b)** imaginary part of the eigenfunctions associated to the critical mode for $n_c = 0.5$ and different values of λ: (1) $\lambda = 0$, Newtonian; (2) $\lambda = 1$; (3) $\lambda = 100$.

where $\langle . \rangle_{xy} = \int_0^{2\pi/\alpha} \int_0^1 (.) dy dx$, u_1 and v_1 are the streamwise and the wall-normal velocities of the fundamental mode. The first term in the right-hand-side, due to dissipation, is always negative. The second term is positive, since the waves extract energy from the basic shear flow, near the wall where the separatrices slope. The third term arises from the viscosity perturbation. It is definite positive, because $\mu_b > \mu_t$ for shear-thinning fluids. It traduces a reduction of the viscous dissipation and may be viewed as an energy source term. It increases when the difference between the effective and the tangent viscosities, *i.e.* increases, with increasing shear-thinning effects. The onset of instability is then found earlier than in the case where the viscosity perturbation is not taken into account.

5.3. *Modification of the mean flow*

As for the linear problem, equation (4.8) with the associated boundary conditions (4.9) is solved numerically using a spectral collocation method based on Chebyshev-polynomials. Figure 8 shows the modification of the mean flow at order $|A|^2$ for two sets of rheological parameters, $\lambda = 10$ and different values of n_c and $n_c = 0.5$ and different values of

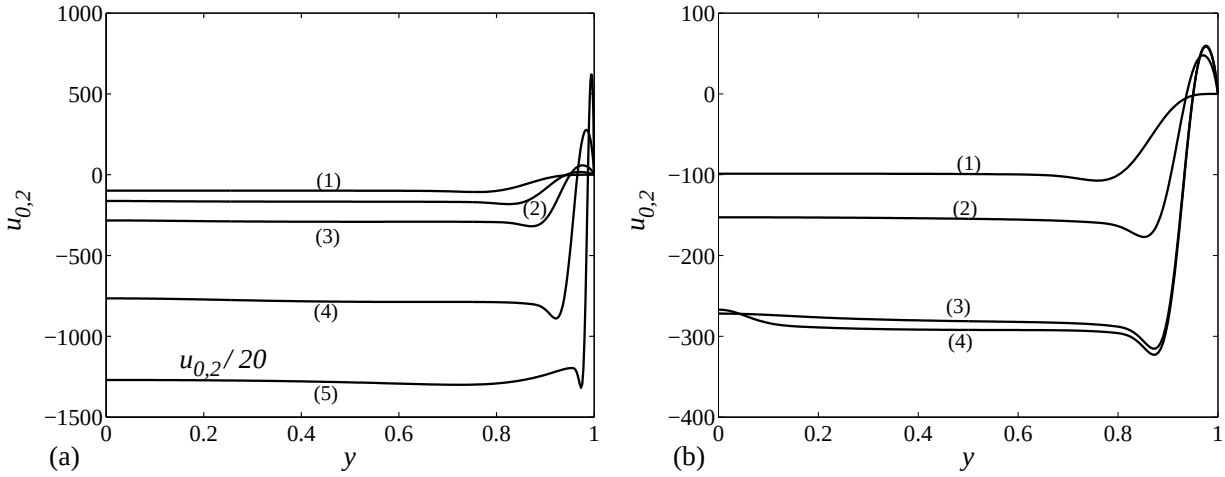

FIGURE 8. Modification of the base flow. **(a)** $\lambda = 10$ and (1) $n_c = 1$ Newtonian; (2) $n_c = 0.7$; (3) $n_c = 0.5$; (4) $n_c = 0.3$; (5) $n_c = 0.1$, for this case, we have represented $u_{0,2}/20$ rather than $u_{0,2}$. **(b)** $n_c = 0.5$ and (1) $\lambda = 0$ Newtonian; (2) $\lambda = 1$; (3) $\lambda = 10$; (4) $\lambda = 100$.

λ. By comparison with the Newtonian case (curve 1), a remarkable difference is that the fluid can be accelerated near the wall. It is always significantly decelerated in the central zone. With increasing shear-thinning effects, the acceleration becomes stronger and more confined near the wall. Canceling artificially the nonlinear viscous terms in (4.8) allows to highlight the contribution of the inertial terms on the modification of the mean flow and vice-versa, to highlight the contribution of the nonlinear viscous terms. The results, shown in figure 9, prove that the interaction of the fundamental with its complex conjugate through nonlinear viscous terms, accelerates the fluid in all the width between the two plates (curves 4 in figure 9). In contrast, the inertial terms reduce the flow rate as for a Newtonian fluid (curves 3 in figure 9).

In order to interpret these results, equation (4.7) is integrated once, and because of the symmetry of u_{02} and $f_{1,1}$ under $y \longmapsto -y$, we obtain

$$\frac{1}{Re}\,\mu_t\, Du_{0,2} = \langle u_1 v_1 \rangle_x - \langle \tau_{2,xy} \rangle_x \,. \tag{5.3}$$

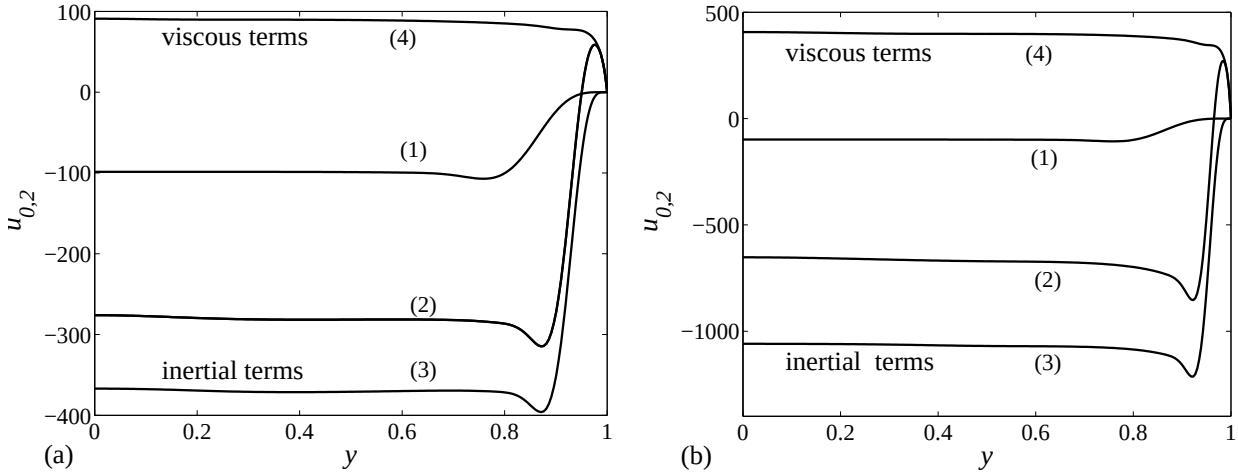

FIGURE 9. Modification of the base flow: **(a)** $n_c = 0.5$ and $\lambda = 10$; **(b)** $n_c = 0.3$ and $\lambda = 10$. (1) Reference curve, Newtonian fluid; (2) Carreau fluid; (3) Carreau fluid with the nonlinear inertial terms only; (4) Carreau fluid with the nonlinear viscous terms only.

The first term on the right-hand of the above equation can be related to the slope x_s' of the separatrices represented in figure 5b via the relation $\langle u_1 v_1 \rangle_x = \langle v_1^2 \rangle_x \, x_s'$ (Plaut *et al.* 2008). The numerical results show that $\langle u_1 v_1 \rangle_x$ is of the sign of $-dU_b/dy$, and increases in magnitude, in the critical layer, with increasing shear-thinning effects. Therefore, the strong deceleration of the flow illustrated by the curves 3 in figures 9(a) and 9(b) can be explained by the increase of the Reynolds-stress. The numerical results show also that $\langle \tau_{2,xy} \rangle_x$, the viscous shear-stress arising from the interaction of the fundamental with its complex conjugate, is positive and increases with increasing the shear-thinning effects. This can explain the acceleration of the flow, induced by the nonlinear viscous terms, illustrated by the curves 4 in figures 9(a) and 9(b). The term on left-hand side of (5.3), *i.e.*, $(1/Re)\mu_t \, (du_{02}/dy) = \tau_{1,xy}$ involves the tangent viscosity $\mu_t < \mu_b$ which amplifies the accelerations and decelerations of the flow described above.

Alternatively, fixed flow rate conditions can be imposed. In this case, a correction $\tilde{P}_{0,2}\, x$ to the pressure field is introduced at order $|A|^2$ such that the modified mean-flow correction

$\tilde{u}_{0,2}$ satisfies

$$\langle \tilde{u}_{0,2}\,(y)\rangle_y = 0. \tag{5.4}$$

The streamwise component of the mean momentum equation at order $|A|^2$ reads

$$\frac{d}{dy}\,(uv)_{0,2} = -\frac{d\tilde{P}_{0,2}}{dx} + \frac{1}{Re}\frac{d}{dy}\left[\mu_t \frac{d\tilde{u}_{0,2}}{dy}\right] + \frac{d}{dy}\,(\tau_{2xy})_{0,2} \tag{5.5}$$

which, by comparison with (4.8) gives

$$\tilde{u}_{0,2}(y) = u_{0,2}(y) - Re\frac{d\tilde{P}_{0,2}}{dx}\int_y^1 \frac{\zeta}{\mu_t}\mathrm{d}\zeta \quad \text{with} \quad \frac{d\tilde{P}_{0,2}}{dx} = \frac{1}{Re}\,\frac{\int_0^1 u_{0,2}(y)dy}{\int_0^1\int_y^1(\zeta/\mu_t)\mathrm{d}\zeta dy} \tag{5.6}$$

All the integrals are evaluated numerically using Clenshaw and Curtis method. The mean flow correction $\tilde{u}_{0,2}$ is shown in figure 10 for fixed λ and different values of n_c. With increasing shear-thinning effects, the flow is accelerated in a thin region adjacent to the wall, followed by a deceleration and then a slight acceleration in a large region around the axis. The fact that the mean pressure gradient $d\tilde{P}_{0,2}/dx$ is negative as it is shown in the figure 10(b) signifies that at fixed flow rate, the transition to generalized Tollmien-Schlichting waves is accompanied by an increase of the head loss. The figure 10(b) suggests also that there is an optimal values of the rheological parameters for which the increase of the head loss is minimum and lower than in the Newtonian case.

5.4. *First harmonic of the fundamental*

Equation (4.10) with the associated boundary conditions (4.11) is solved using the same numerical approach as in §5.3. The first harmonic of the fundamental which has half its wavelength is displayed in figure 11 for a Carreau fluid with $\lambda = 10$ and $n_c = 0.3$. The real and the imaginary parts of $f_{2,2}$ are shown in figure 12 for $\lambda = 10$ and different values of n_c. It is observed that shear-thinning induces a significant amplification of $f_{2,2}$. To determine the contribution of the inertial terms to the generation of the first harmonic, the nonlinear viscous terms in the r.h.s. of equation (4.10) are canceled artificially, and

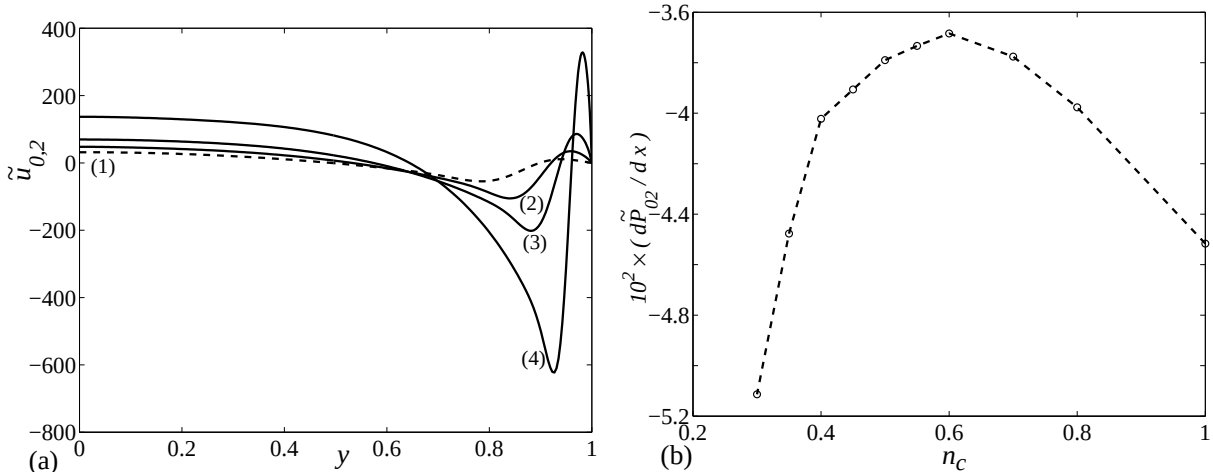

FIGURE 10. **(a)** Modification of the base flow for fixed flow rate at $\lambda = 10$ and different n_c: (1) Reference curve obtained for Newtonian fluid and represented by the dashed line; (2) $n_c = 0.7$; (3) $n_c = 0.5$; (4) $n_c = 0.3$. **(b)** Correction to the mean pressure gradient versus n_c at fixed flow rate and $\lambda = 10$.

vice-versa to obtain the contribution of the quadratic nonlinearity arising from the viscosity. The results are shown in figure 13. It appears that the first harmonic generated by the nonlinear viscous terms is smaller and in opposite phase with that generated by the quadratic nonlinear inertial terms. This reveals probably, that the mechanism of energy exchange between the fundamental and its harmonic via the nonlinear inertial terms is different compared to that via the nonlinear viscous terms.

5.5. *Cubic Landau constant*

The cubic coefficient g_1, *i.e.*, the first Landau constant in (4.5) is determined for different critical sets $(n_c, \lambda, Re, \alpha)$. The integrals in (4.14)-(4.16) are evaluated numerically by means of Clenshaw and Curtis Method. In figure 14(a), we plot $g_{1r} = \mathcal{R}e\,(g_1)$ in terms of λ for fixed values of n_c. As one could expect, the sign of g_{1r} is found positive indicating a subcritical bifurcation. For fixed n_c, g_{1r} increases as the dimensionless characteristic time λ increases and tends towards an asymptote. In the same way, for a given λ, g_{1r}

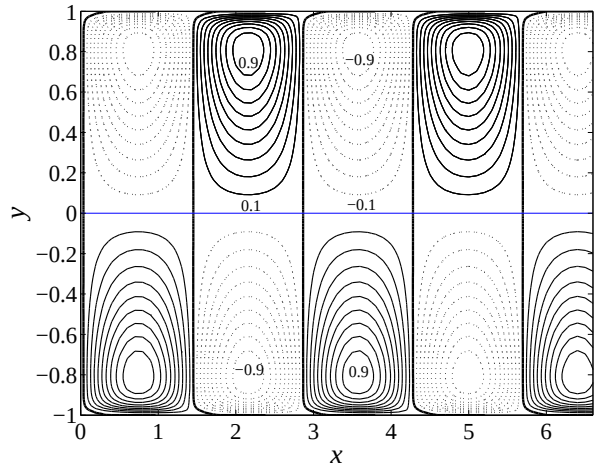

FIGURE 11. Iso-values of $\mathcal{R}e\left(f_{2,2}E^2\right)$ at the critical conditions and $t = 0$, for a Carreau-fluid with $\lambda = 10$ and $n_c = 0.3$. Continuous and dotted lines correspond respectively to positive and negative values of $\mathcal{R}e\left(f_{2,2}E^2\right)$. They are normalized by the maximum value and displayed by step of 0.1.

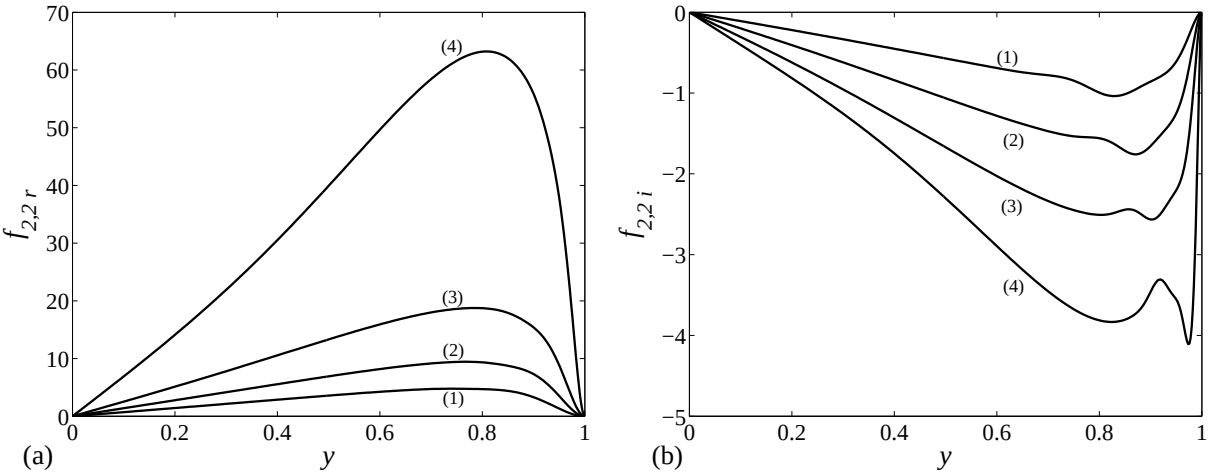

FIGURE 12. Real **(a)** and imaginary **(b)** parts of the first harmonic of the critical mode for $\lambda = 10$ and different values of the shear-thinning index n_c: (1) $n_c = 1$ Newtonian case; (2) $n_c = 0.7$; (3) $n_c = 0.5$; (4) $n_c = 0.3$.

increases strongly as n_c decreases. Thus shear-thinning effects, while tending to promote stability on a linear basis, also tend to augment the subcritical character of the bifurcation. Contributions of the different terms g_{10}^I, g_{12}^I, g_{10}^V, ... (see equation 4.13) that control

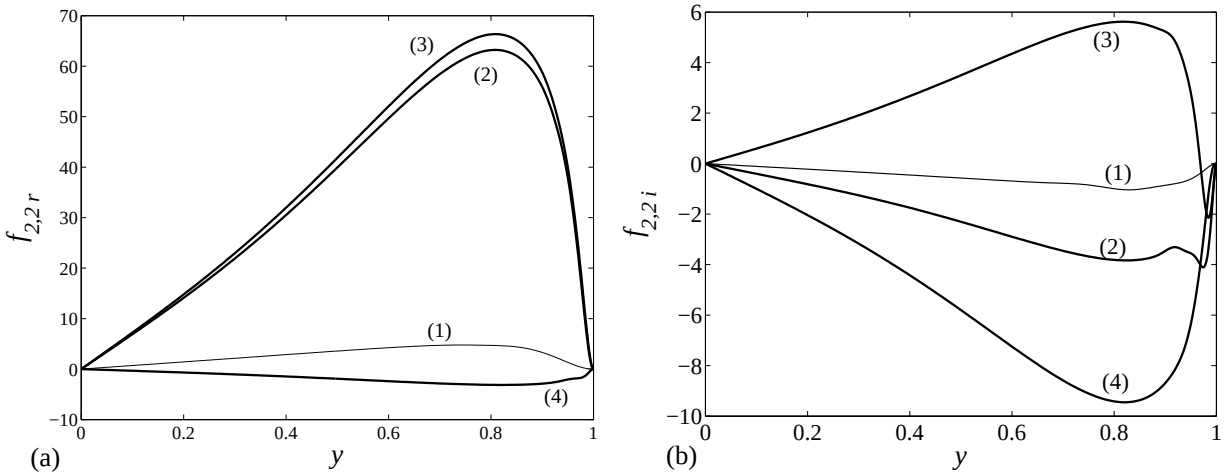

FIGURE 13. Real **(a)** and imaginary **(b)** parts of the first harmonic of the fundamental mode at the critical condition for Carreau fluid with $\lambda = 10$ and $n_c = 0.3$. (1) $n_c = 1$ Newtonian case as a reference curve; (2) Carreau fluid ; (3) Carreau fluid: contribution of the inertial terms; (4) Carreau fluid: contribution of the nonlinearities arising from the viscous terms.

the value of g_{1r} are given in tables 2 and 3 for fixed pressure gradient and fixed flow rate respectively. The data show that with increasing shear-thinning effects, the feedback of the harmonic onto the waves plays an important role in the subcritical bifurcation, whilst in the Newtonian case g_{12}^I is negative and the subcritical nature of the bifurcation is due to the feedback of the mean flow correction onto the wave (Reynolds & Potter 1967; Plaut *et al.* 2008).

If the nonlinear viscous terms are canceled artificially in the disturbance equation (2.31), higher values of g_{1r} are found. This can be assessed by comparing curve (2) obtained without nonlinear viscous terms and curve (3) in figure 14(b). For $\lambda \geqslant 10$, the relative difference is about 20%. In contrast, if the nonlinear inertial terms are canceled in the disturbance equation (2.31), g_{1r} is negative and the bifurcation becomes supercritical (see the curve 4 of figure 14. Hence, for shear-thinning fluids, the nonlinear variation of μ with the shear-rate favors a supercritical bifurcation.

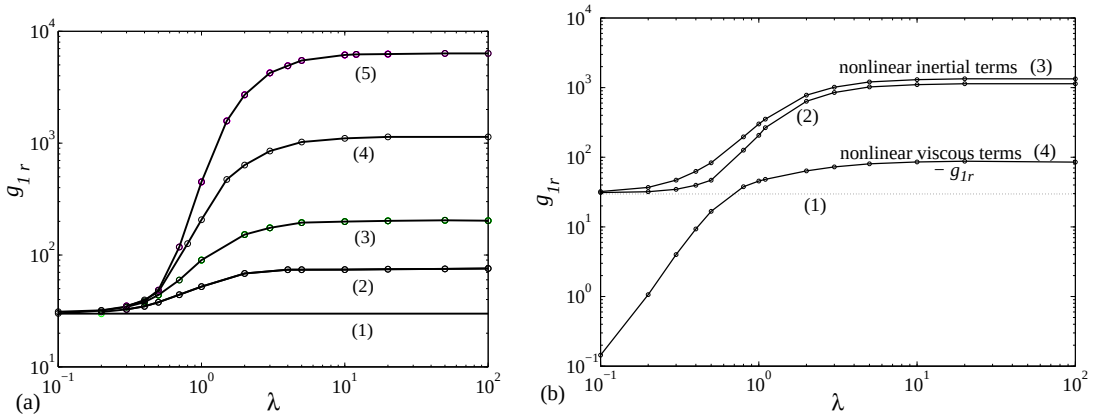

FIGURE 14. **(a)** Real part of the Landau constant as function of λ and different values of n_c, under the fixed pressure-gradient condition. (1) Newtonian case $n_c = 1$; (2) $n_c = 0.7$; (3) $n_c = 0.5$; (4) $n_c = 0.3$; (5) $n_c = 0.2$. **(b)** Real part of the Landau constant versus λ for a given shear-thinning index $n_c = 0.3$. (1) Newtonian fluid, (2) Carreau fluid, (3) Only nonlinear inertial terms are retained and (4) Only nonlinear viscous terms are retained; in this case the opposite of g_{1r} is shown

n_c	g_{1r}	g^I_{10}	g^V_{10}	g^I_{12}	g^V_{12}	g^V_{1-11}
1	29.72	39.48	0	-9.76	0	0
0.7	74.16	78.71	-3.44	-9.85	6.19	2.55
0.5	206.437	168.830	-11.34	12.613	32.468	3.860
0.4	428.068	288.250	-24.854	77.590	78.214	8.859
0.3	1211.231	613.329	-66.187	384.93	251.372	27.772
0.2	6391.031	2076.469	-137.864	3010.636	1467.892	118.363

TABLE 2. Fixed pressure gradient condition. Real part of the first Landau constant and contribution of the nonlinear inertial and nonlinear viscous terms, for different values of the shear-thinning index at $\lambda = 10$. For the Newtonian case, the value of g_{1r} is in agreement with that given by Reynolds & Potter (1967).

n_c	g_{1r}	g_{10}^I	g_{10}^V	g_{12}^I	g_{12}^V	g_{1-11}^V
1	30.95	40.73	0	-9.791	0	0
0.7	78.42	81.40	-2.59	-9.271	7.95	0.92
0.5	198.87	163.51	-12.78	12.27	25.85	10.02
0.4	409.76	278.15	-27.06	74.24	62.67	21.75
0.3	1162.59	592.45	-69.89	376.07	206.34	57.61
0.2	6082.85	1979.84	-285.24	2890.39	1258.07	239.75

TABLE 3. Same as table 2 but for fixed flow rate condition. For the Newtonian case, the value of g_{1r} is in agreement with that given by Fujimura (1989).

5.6. *Threshold amplitude*

Beside the Landau coefficient, the threshold amplitude, $|A_c|$, which limits the basin of attraction of undisturbed parallel flow, is another important quantity in the nonlinear stability analysis. It is obtained by setting $dA/dt = 0$ in (4.5): the linear growth rate and its nonlinear correction balance. In the neighborhood of the critical conditions such that $(Re_c - Re)/Re_c = \epsilon << 1$, using Taylor expansion, αc_i can be written as $\alpha\, c_i = \epsilon/\tau_0 + O(\epsilon^2)$, where the τ_0 is a characteristic time. Hence, to lowest order in ϵ, the threshold amplitude is

$$|A_c| = \sqrt{\frac{\epsilon}{\tau_0\ g_{1r}}}. \tag{5.7}$$

One has to note that $(\mathrm{d}c_i/\mathrm{d}\epsilon)_{\epsilon=0}$ has to be evaluated for a given fluid and flow geometry that is for a constant $\Lambda = \lambda/[Re_c\ (1-\epsilon)]$. Figure 15(a) shows the threshold amplitude in the form $|A_c|/\sqrt{\epsilon}$ as a function of the shear-thinning index n_c. The curve illustrates that the flow becomes much more sensitive to small disturbances since the threshold

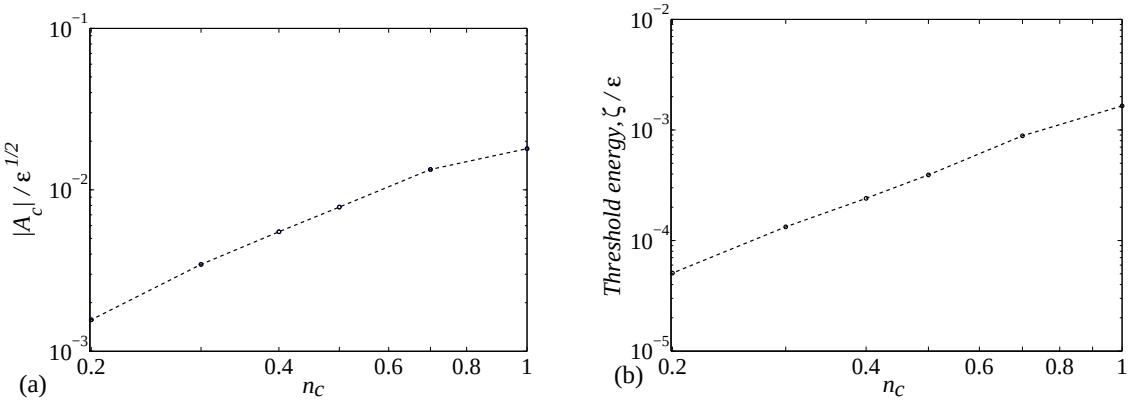

FIGURE 15. Fixed pressure gradient condition. **(a)** Scaled threshold amplitude, beyond which the flow is nonlinearly unstable, as function of n_c at $\lambda = 100$. **(b)** Threshold kinetic energy as a function of the shear-thinning index, n_c at $\lambda = 100$.

amplitude significantly decreases as the shear-thinning effects increase, *i.e.*, the flow becomes relatively more nonlinearly unstable. The numerical results indicate also that the characteristic time τ_0 decreases. For instance, for a Newtonian fluid, we have $\tau_0 = 103.1$, in agreement with Herbert (1980), compared to 63.11 obtained for a Carreau fluid with $n_c = 0.2$ and $\lambda = 100$. One has to note that the numerical values of the Landau constant and hence the values of A_c depend upon the normalization condition used for the eigenfunctions in the linear theory. However, the physical velocity components, i.e. the product of the amplitude with the eigenfunctions of the linear theory are independent of the normalization. For instance, we can consider the threshold kinetic energy required for a finite amplitude instability, defined by

$$\zeta = 2\,|A_c|^2 \int_0^1 \left[|Df_{1,1}|^2 + \alpha_c^2\,|f_{1,1}|^2\right]\, dy. \tag{5.8}$$

Figure 15(b) plots the threshold kinetic energy in the form ζ/ϵ as a function of the shear-thinning index n_c, for $\lambda = 100$. As it can be observed, the threshold kinetic energy decreases significantly as n_c decreases, highlighting the destabilizing effect of shear-thinning for finite amplitude perturbations.

5.7. *Validation by computing higher-order Landau constants*

Figure 15 indicates that the threshold amplitude beyond which the flow is nonlinearly unstable decreases with increasing shear-thinning effects. This result was obtained by truncating the series (4.5) to the first Landau constant, at cubic order in A. For a significant deviation from the critical condition, terms of higher order become large and should be taken into account. Weakly nonlinear expansion was then carried out up to seventh order in amplitude under fixed flow rate condition. For the sake of clarity, calculation details are not given in the text, (see Appendix C). As in the Newtonian case, for shear-thinning fluids, the real part of Landau constants are of alternating sign and increase very fast. This increase is stronger with increasing shear-thinning effects as is shown by the data in table 4. Figure 16 shows the evolution of the threshold amplitude $|A_c|$ versus the relative departure from the critical conditions, $\epsilon = (Re_c - Re)/Re_c$, for different values of the shear-thinning index. The results are presented at cubic, fifth and seventh order in the amplitude expansion. At $n_c = 0.3$, the three curves (cubic, fifth and seventh order) are not distinguishable within plotting accuracy. At $\epsilon = -0.05$, the relative difference in $|A_c|$ between the fifth and the seventh order is 0.6% for $n_c = 0.3$ and 4.6% for a Newtonian fluid. The threshold amplitude decreases with increasing shear-thinning effects. This result is valid at least for a reasonable relative departure from the critical conditions.

6. Conclusion

The present work focuses on the first principles understanding of the influence of shear-thinning effects on the flow stability with respect to finite amplitude perturbations. The fluid is supposed purely viscous. Hence, in presence of a perturbation $\boldsymbol{u}$, it is assumed that the viscosity instantaneously adjusts the shear rate of the perturbed flow

n_c	g_{1r}	g_{2r}	g_{3r}
1	30.95	-3.00×10^5	6.78×10^9
$1'$	30.95	-3.00×10^5	6.39×10^9
0.7	78.42	-1.62×10^6	9.27×10^{10}
0.5	198.87	-9.52×10^3	1.30×10^{12}
0.3	1.17×10^3	-2.09×10^8	9.77×10^{13}

TABLE 4. Real part of the Landau constants for different values of the shear-thinning index at $\lambda = 10$. For the Newtonian case, the values of g_{1r}, g_{2r} and g_{3r} are in good agreement with that given by Fujimura (1989), for fixed flow rate condition, and reported here on the line $1'$.

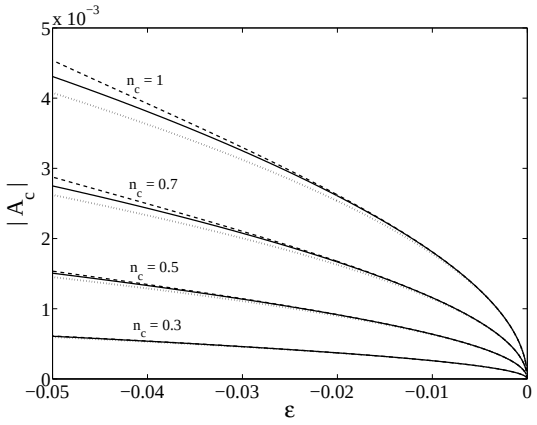

FIGURE 16. Threshold amplitude vs $\epsilon = (Re_c - Re)/Re$ for different values of the shear-thinning index, under the condition of fixed flow rate. The truncation levels of the Stuart-Landau equation are also provided: (dotted line) cubic order, (dashed line) fifth order, (continuous line) seventh-order.

$\boldsymbol{U}_b + \boldsymbol{u}$. Physically, this assumes that the characteristic time of the reorganization of the internal structure is much smaller than the characteristic time of the perturbation. In the case, where the reorganization time of the internal structure has to be considered, a

thixotropic model for the viscosity has to be used. In such a model, the internal structure is defined using a single parameter. The behaviour of this parameter is determined by a phenomenological kinetic process. To our knowledge, even the linear stability analysis of channel flows of thixotropic fluids has not yet been performed. One of the difficulties arises from the fact that several thixotropic models are not structurally stable (Billingham & Ferguson 1993).

Compared to the Newtonian case, an additional nonlinearity appears in the momentum equations, via the rheological law of the fluid. This additional nonlinearity is not analytical and thus more complex than the quadratic nonlinear inertial terms. A weakly nonlinear analysis of the bifurcation to two-dimensional generalized Tollmien-Schlichting waves is used as a first approach to take into account nonlinear effects. The amplitude expansion method of Landau and Stuart is adopted. The Carreau model is used as a typical rheological model of shear-thinning fluids. The main conclusions of the analysis are: (i) At order $|A|^2$, when a constant pressure drop is imposed, the nonlinear viscous terms reduce the viscous dissipation and tend to accelerate the fluid while the nonlinear inertial terms reduce the flow rate. These modifications of the mean flow increase with increasing shear-thinning effects. (ii) The harmonic generated by the nonlinearity $\mu(\dot{\gamma})$, is smaller and in opposite phase with that generated by the quadratic nonlinear inertial terms. The modulus of the harmonic increases with increasing shear-thinning effects. (iii) The real part of the cubic Landau constant g_{1r} becomes large and positive as n_c decreases or as λ increases. Thus, shear-thinning effects, while tending to promote stability on the basis of the linear theory (Chikkadi *et al.* 2005; Nouar *et al.* 2007), also tend to increase highly the subcritical nature of the bifurcation. If the nonlinear viscous terms are canceled artificially, higher values of g_{1r} are found. In contrast, if the nonlinear inertial terms are canceled, g_{1r} is negative and the bifurcation becomes supercritical.

Beside the Landau constant, the threshold amplitude of the bifurcation which limits the basin of attraction of the laminar flow was determined. Because of higher values of g_{1r}, the threshold amplitude decreases with increasing shear-thinning. This result was confirmed by computing higher order Landau constants.

In order to compute nonlinear waves far below onset, the technique used here will become prohibitively tedious (see Appendix C) when higher order terms in Landau equation are included. A fully numerical method, *e.g.*, a continuation method based on Euler-Newton and pseudo-spectral methods, would be quite useful for this purpose.

One Referee has drawn our attention to an interesting point. For sufficiently large amplitude of the primary wave, the mean velocity profile $U_b + |A_p|^2 u_{0,2}$ may exhibit an inflection point near the wall (see figure 8), that could lead to an instability through an inviscid mechanism (Rayleigh and Fjortoft theorems). The numerical results show that the critical amplitude above which an inflectional velocity profile is obtained decreases with increasing shear-thinning effects. This critical amplitude is one order of magnitude larger than the values given in figure 16. The study of such secondary instabilities and of three-dimensional instabilities will be relevant.

It is worthy to note that in Rayleigh-Bénard convection of shear-thinning fluids, a tendency towards subcritical bifurcations when shear-thinning effects are introduced has been evidenced by Balmforth & Rust (2009); Albbalbaki & Khayat (2011). This tendency is in line with our results, though the physical mechanisms of the instabilities are different. It is probably a generic feature of instabilities in shear-thinning fluids.

Appendix A. The linear (L_k), bilinear (N_I and N_{vquad}) and trilinear (N_{vcub}) involved in the differential equations for $f_{k,\ell}$

The ordinary differential equations for the function $f_{k,\ell}$, involve the following linear (L_k), bilinear (N_I and N_{vquad}) and trilinear forms (N_{vcub}):

$$\begin{aligned} L_k\, f_{k,\ell} = & -i\, k\, \alpha\, c_c\, S_k\, f_{k,\ell} - i\, k\, \alpha\, \left(D^2 U_b - U_b\, S_k\right)\, f_{k,\ell} \\ & - \frac{1}{Re}\, \mu_b\, S_k^2\, f_{k,\ell} - \frac{1}{Re}\, \left[D^2 \mu_b\, \mathcal{G}_k\, + 2\, (D\mu_b)\, S_k\, D\right] f_{k,\ell} \\ & - \frac{1}{Re} \mathcal{G}_k\, \left[(\mu_t - \mu_b)\, \mathcal{G}_k\, f_{k,\ell}\right]. \end{aligned} \tag{A 1}$$

One can notice that the linear problem $L_1 f_{1,1} = 0$ is the Orr-Sommerfeld equation.

$$N_I\,(f_{n,p}, f_{m,q}) = i\, n\, \alpha\, f_{n,p}\, S_m\, D f_{m,q} - i\, \alpha\, m\, D f_{n,p}\, S_m\, f_{m,q}. \tag{A 2}$$

$$N_I\,(f_{n,p} | f_{m,q}) = N_I\,(f_{n,p}, f_{m,q}) + N_I\,(f_{m,q}, f_{n,p}) \tag{A 3}$$

$$\begin{aligned} Re\, N_{Vquad}\,(f_{n,p}, f_{m,q}) = & -8\alpha^2\, m\,(n+m)\, D\left[\dot{\gamma}_{xy}^b\, \left.\frac{\partial \mu}{\partial \Gamma}\right|_b\, (\mathcal{G}_n\, f_{n,p})\, (D f_{m,q})\right] \\ & + \mathcal{G}_{(n+m)}\, \left[3\, \dot{\gamma}_{xy}^b\, \left.\frac{\partial \mu}{\partial \Gamma}\right|_b\, (\mathcal{G}_n\, f_{n,p})\, (\mathcal{G}_m\, f_{m,q})\right] \\ & + \mathcal{G}_{(n+m)}\, \left[2\, \left(\Gamma\, \frac{\partial^2 \mu}{\partial \Gamma^2}\right)_b\, \dot{\gamma}_{xy}^b\, (\mathcal{G}_n f_{n,p})\, (\mathcal{G}_m f_{m,q})\right] \\ & + \mathcal{G}_{(n+m)}\, \left[-4\, \alpha^2\, n\, m\, \dot{\gamma}_{xy}^b\, \left.\frac{\partial \mu}{\partial \Gamma}\right|_b\, (D f_{n,p})\, (D f_{m,q})\right], \end{aligned} \tag{A 4}$$

$$N_{Vquad}\,(f_{n,p} | f_{m,q}) = N_{Vquad}\,(f_{n,p}, f_{m,q}) + N_{Vquad}\,(f_{m,q}, f_{n,p})\,. \tag{A 5}$$

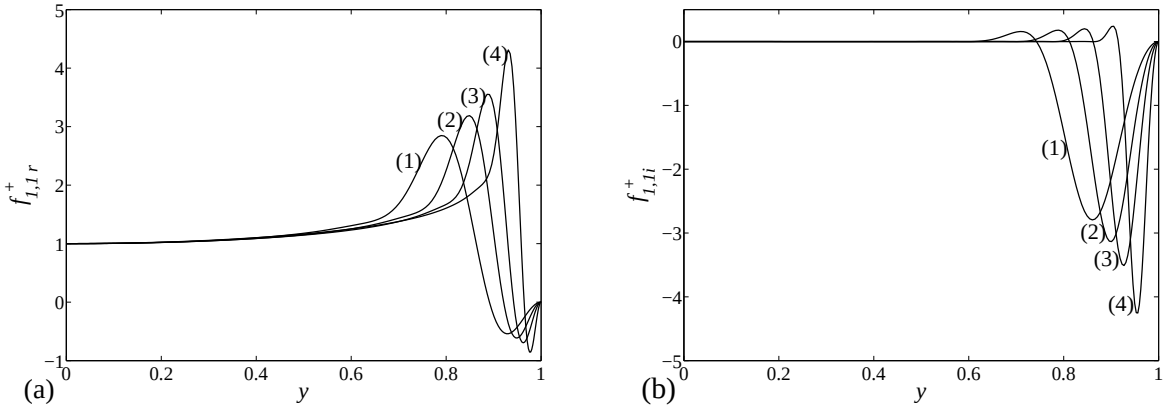

FIGURE 17. Real (a) and imaginary (b) parts of the eigenfunction of the adjoint linear operator at $\lambda = 10$ and different shear-thinning index: (1) Newtonian, (2) $n_c = 0.7$, (3) $n_c = 0.5$ and (4) $n_c = 0.3$. (a) Real part and (b) imaginary part.

$$
\begin{aligned}
Re\, N_{Vcub} = {} & (n+m+k)\ \alpha\, D\ \left[16 n\, m\, k\, \alpha^3\ \left.\frac{\partial \mu}{\partial \Gamma}\right|_b\ (Df_{n,p})\ (Df_{m,q})\ (Df_{k,\ell})\right] \\
& + (n+m+k)\ \alpha\, D\ \left[-4\alpha\, k\ \left(\frac{\partial \mu}{\partial \Gamma} + 2\Gamma \frac{\partial^2 \mu}{\partial \Gamma^2}\right)_b\ (\mathcal{G}_n f_{n,p})\ (\mathcal{G}_m f_{m,q})\ (Df_{k,\ell})\right] \\
& + \mathcal{G}_{(n+m+k)}\ \left[-4\, n\, m\, \alpha^2\ \left.\frac{\partial \mu}{\partial \Gamma}\right|_b\ (Df_{n,p})\ (Df_{m,q})\ (\mathcal{G}_k f_{k,\ell})\right] \\
& + \mathcal{G}_{(n+m+k)}\ \left[\left(\frac{\partial \mu}{\partial \Gamma} + 2\,\Gamma\, \frac{\partial^2 \mu}{\partial \Gamma^2}\right)_b\ (\mathcal{G}_n f_{n,p})\ (\mathcal{G}_m f_{m,q})\ (\mathcal{G}_k f_{k,\ell})\right] \\
& + \mathcal{G}_{(n+m+k)}\ \left[-8\alpha^2\, n\, m\, \Gamma_b\ \left.\frac{\partial^2 \mu}{\partial \Gamma^2}\right|_b\ (Df_{n,p})\ (Df_{m,q})\ (\mathcal{G}_k f_{k,\ell})\right] \\
& + \mathcal{G}_{(n+m+k)}\ \left[2\,\Gamma_b\ \left(\frac{\partial^2 \mu}{\partial \Gamma^2} + \frac{2}{3}\Gamma\, \frac{\partial^3 \mu}{\partial \Gamma^3}\right)_b\ (\mathcal{G}_n f_{n,p})\ (\mathcal{G}_m f_{m,q})\ (\mathcal{G}_k f_{k,\ell})\right] \qquad \text{(A 6)}
\end{aligned}
$$

$$
\begin{aligned}
N_{Vcub}\,(f_{n,p}, f_{m,q} | f_{k,\ell}) = {} & N_{Vcub}\,(f_{n,p}, f_{m,q}, f_{k,\ell}) + N_{Vcub}\,(f_{k,\ell}, f_{n,p}, f_{m,q}) \\
& + N_{Vcub}\,(f_{m,q}, f_{k,\ell}, f_{n,p}) \qquad \text{(A 7)}
\end{aligned}
$$

Appendix B. Adjoint eigenmode

The eigenfunctions of the adjoint linear operator for different values of the shear index n_c are displayed in figure 17.

Appendix C. Expansion to seventh-order

To evaluate the Landau constant up to seventh order in amplitude, viscosity of the perturbed flow needs to be expanded, around the base flow, up to seventh order:

$$\mu(\Psi_b+\psi)=\mu_b+\mu_1+\mu_2+...+\mu_7+.... \tag{C 1}$$

with

$$\mu_4=\frac{2}{3}\left.\frac{\partial^4\mu}{\partial\Gamma^4}\right|_b\left(\dot\gamma_{xy}^b\right)^4\left(\dot\gamma_{xy}\right)^4(\psi)+2\,\frac{\partial^3\mu}{\partial\Gamma^3}\,\Gamma_b\,\dot\gamma_{xy}^2(\psi)\,\Gamma_2+\frac{1}{2}\left.\frac{\partial^2\mu}{\partial\Gamma^2}\right|_b\Gamma_2 \tag{C 2}$$

$$\begin{aligned}\mu_5=&\frac{4}{15}\left.\frac{\partial^5\mu}{\partial\Gamma^5}\right|_b\left(\dot\gamma_{xy}^b\right)^5\left(\dot\gamma_{xy}\right)^5(\psi)+\frac{4}{3}\left.\frac{\partial^4\mu}{\partial\Gamma^4}\right|_b\left(\dot\gamma_{xy}^b\right)^3\left(\dot\gamma_{xy}\right)^3(\psi)\,\Gamma_2\\&+\left.\frac{\partial^2\mu}{\partial\Gamma^2}\right|_b\dot\gamma_{xy}^b\,\dot\gamma_{xy}(\psi)\,\Gamma_2^2,\end{aligned} \tag{C 3}$$

$$\begin{aligned}\mu_6=&\frac{4}{5}\left.\frac{\partial^6\mu}{\partial\Gamma^6}\right|_b\left(\dot\gamma_{xy}^b\right)^6\left(\dot\gamma_{xy}\right)^6(\psi)+\frac{2}{3}\left.\frac{\partial^5\mu}{\partial\Gamma^5}\right|_b\left(\dot\gamma_{xy}^b\right)^4\left(\dot\gamma_{xy}\right)^4(\psi)\,\Gamma_2\\&+\left.\frac{\partial^4\mu}{\partial\Gamma^4}\right|_b\left(\dot\gamma_{xy}^b\right)^2\left(\dot\gamma_{xy}\right)^2(\psi)\,\Gamma_2^2+\frac{1}{6}\left.\frac{\partial^3\mu}{\partial\Gamma^3}\right|_b\Gamma_2^3\end{aligned} \tag{C 4}$$

$$\begin{aligned}\mu_7=&\frac{8}{315}\left.\frac{\partial^7\mu}{\partial\Gamma^7}\right|_b\left(\dot\gamma_{xy}^b\right)^7\left(\dot\gamma_{xy}\right)^7(\psi)+\frac{2}{3}\left.\frac{\partial^5\mu}{\partial\Gamma^5}\right|_b\left(\dot\gamma_{xy}^b\right)^3\left(\dot\gamma_{xy}\right)^3(\psi)\,\Gamma_2^2\\&+\frac{1}{3}\left.\frac{\partial^4\mu}{\partial\Gamma^4}\right|_b\dot\gamma_{xy}^b\,\dot\gamma_{xy}(\psi)\,\Gamma_2^3.\end{aligned} \tag{C 5}$$

The deviatoric stresses of disturbed flow are written as:

$$\tau_{ij}(\Psi_b+\psi)=\tau_{ij}(\Psi_b)+\tau_{1,ij}+\tau_{2,ij}+...+\tau_{7,ij}+..., \tag{C 6}$$

where

$$\tau_{k,ij}=\mu_{k-1}\,\dot\gamma_{ij}+\mu_k\,\dot\gamma_{ij}^b\qquad;\qquad k\geqslant 2. \tag{C 7}$$

At order k, the nonlinear viscous term in the perturbation equation (2.31) is therefore

$$\begin{aligned}Re\,\mathcal{N}_{V\,k}(\psi,...,\psi)=&\frac{\partial^2}{\partial x\partial y}\left[\mu_{k-1}\left(\dot\gamma_{xx}(\psi)-\dot\gamma_{yy}(\psi)\right)\right]\\&+\left(\frac{\partial^2}{\partial y^2}-\frac{\partial^2}{\partial x^2}\right)\left[\mu_{k-1}\dot\gamma_{xy}(\psi)+\mu_k\,\dot\gamma_{xy}(\Psi_b)\right].\end{aligned} \tag{C 8}$$

Finally, the method for obtaining the Landau constants g_j is to impose the solvability condition on the equation for $f_{1,j}$ (distortion of the fundamental mode). The normaliza-

tion condition $f_{1,j} = 0$ at $y = 0$ for $j > 1$ is used in order to guarantee the uniqueness of solutions (Herbert 1983; Fujimura 1989).

REFERENCES

Albbalbaki, B. & Khayat, R.E. 2011 Pattern selection in the thermal convection of non-newtonian fluids. *J. Fluid Mech* **668**, 500–550.

Balmforth, N. J. & Rust, A. C. 2009 Weakly nonlinear viscoplastic convection. *J. Non-Newtonian Fluid Mech.* **158**, 36–45.

Billingham, J. & Ferguson, J. W. J. 1993 Laminar, unidirectional flow of a thixotropic fluid in a circular pipe . *J. Non-Newtonian Fluid Mech.* **47**, 21–55.

Bird, R., Amstrong, R. & Hassager, O. 1987 Dynamics of polymeric liquids. Wiley - Interscience, New York.

Carreau, J. P. 1972 Rheological equations from molecular network theories. *J. Rheol.* **16**, 99–127.

Chikkadi, V., Sameen, A. & Govindarajan, R. 2005 Preventing transition to turbulence: A viscosity stratification does not always help. *Phys. Rev. Lett.* **95**, 264504.1–4.

Drazin, P. G. & Reid, W. H. 1995 Hydrodynamic stability. Cambridge University Press.

Ern, P., Charru, F. & Luchini, P. 2003 Stability analysis of a shear flow with strongly stratified viscosity. *J. Fluid Mech.* **496**, 295–312.

Fujimura, K. 1989 The equivalence between two perturbation methods in weakly nonlinear stability theory for parallel shear flows. *Proc. R. Soc. Lond. A* **424**, 373–392.

Govindarajan, R. 2002 Surprising effects of minor viscosity gradients. *J. Indian Inst. Sci.* **82**, 121–127.

Govindarajan, R., L'Vov, V. S., Procaccia, I. & Sameen, A. 2003 Stabilization of hydrodynamic flows by small viscosity variations. *Phys. Rev. E* **67**, 026310.1–11.

Govindarajan, R., L'vov, V. S. & Proccaccia, I. 2001 Retardation of the onset of turbulence by minor viscosity contrasts. *Phys. Rev. Lett.* **87**, 174501.1–4.

Herbert, T. 1980 Nonlinear stability of parallel flows by high-order amplitude expansions. *A.I.A.A.* **18**, 243–248.

Herbert, T. 1983 On perturbation methods in nonlinear stability theory. *J. Fluid Mech.* **126**, 167–186.

Nouar, C., Bottaro, A. & Brancher, J. P. 2007 Delaying transition to turbulence in channel flow: Revisiting the stability of shear-thinning fluids. *J. Fluid. Mech.* **592**, 177–194.

Nouar, C. & Frigaard, I. 2009 Stability of plane Couette-Poiseuille flow of shear-thinning fluid. *Phys. Fluids* **21**, 064104.1–13.

Phillips, G.O. & Williams, P.A. 2000 Handbook of hydrocolloïdes. Woodhead Publishing, Cambridge.

Plaut, E., Lebranchu, Y., Simitev, R. & Busse, F.H. 2008 Reynolds stresses and mean fields generated by pure waves: Applications to shear flows and convection in a rotating cell. *J. Fluid. Mech.* **602**, 303–326.

Quemada, D. 1978 Rheology of concentrated disperse sytem. ii. a model for non-newtonian shear viscosity in steady flows. *Rheol. Acta* **17**, 632–642.

Ranganathan, B. T. & Govindarajan, R. 2001 Stabilization and destabilization of channel flow by location of viscosity-stratified fluid layer. *Phy. Fluids* **13**, 1–3.

Reynolds, W. C. & Potter, M. C. 1967 Finite-amplitude instability of parallel shear flows. *J. Fluid Mech.* **27**, 465–492.

Sameen, A. & Govindarajan, R. 2007 The effect of wall heating on instability of channel flow. *J. Fluid. Mech.* **577**, 417–442.

Schmid, P. J. & Henningson, D. S. 2001 Stability and transition in shear flows. Springer - Verlag.

Stuart, J. T. 1960 On the non-linear mechanics of wave disturbances in stable and unstable parallel flows: Part 1. The basic behaviour in plane Poiseuille flow. *J. Fluid. Mech.* **9**, 353–370.

Tanner, R. 2000 Engineering rheology. Oxford University Press, New York.

Wall, D. P. & Wilson, S. K. 1996 The linear stability of channel flow of fluid with temperature-dependent viscosity. *J. Fluid. Mech.* **323**, 107–132.

Watson, J. 1960 On the non-linear mechanics of wave disturbances in stable and unstable

parallel flows. part 2. The development of a solution for plane Poiseuille and for plane Couette flow. *J. Fluid. Mech.* **9**, 371–389.